This is a postprint of:

[Article begins on next page]

Dissolved aluminium in the Ocean Conveyor of the West Atlantic Ocean:
effects of the biological cycle, scavenging, sediment resuspension and hydrography

R. Middag[a,b] [*], M.M.P. van Hulten[c,d], H.M. Van Aken[a], M.J.A. Rijkenberg[a], L.J.A. Gerringa[a], P. Laan[a], H.J.W. de Baar[a,e]

[a] Royal Netherlands Institute for Sea Research (Royal NIOZ), Den Burg, Texel, the Netherlands.
[b] Department of Chemistry, University of Otago, Dunedin, Otago, New Zealand.
[c] Royal Netherlands Meteorological Institute (KNMI), De Bilt, the Netherlands
[d] Laboratoire des Sciences du Climat et de l'Environnement (LSCE), Gif-sur-Yvette, France
[e] Department of Ocean Ecosystems, University of Groningen, Groningen, the Netherlands

[*]Corresponding Author: Rob Middag, rob.middag@otago.ac.nz, +64 03 479 7907

Co-authors email addresses:
Marco van Hulten (marco.van-hulten@lsce.ipsl.fr)
Hendrik van Aken (hm.vanaken@texel.com)
Micha Rijkenberg (micha.rijkenberg@nioz.nl)
Loes Gerringa (loes.gerringa@nioz.nl)
Patrick Laan (patrick.laan@nioz.nl)
Hein de Baar (hein.de.baar@nioz.nl)

Abstract

The concentrations of dissolved aluminium (dissolved Al) were studied along the West Atlantic GEOTRACES GA02 transect from 64°N to 50°S. Concentrations ranged from ~0.5 nmol kg^{-1} in the high latitude surface waters to ~48 nmol kg^{-1} in surface waters around 25°N. Elevated surface water concentrations due to atmospheric dust loading have little influence on the deep water distribution. However, just below the thermocline, both Northern and Southern Hemisphere Subtropical Mode Water, are elevated in Al, most likely related to atmospheric dust deposition in the respective source regions.

In the deep ocean, high concentrations of up to 35 nmol kg^{-1} were observed in North Atlantic Deep Water as a result of Al input via sediment resuspension. Comparatively low deep water concentrations were associated with water masses of Antarctic origin. During water mass advection, Al loss by scavenging overrules input via remineralisation and sediment resuspension at the basin wide scale. Nevertheless, sediment resuspension is more important than previously realised for the deep ocean Al distribution and even more intensive sampling is needed in bottom waters to constrain the spatial heterogeneity in the global deep ocean.

This thus far longest (17,500 km) full depth ocean section shows that the distribution of Al can be explained by its input sources and the combination of association with particles and release from those particles at depth, the latter most likely when the particles remineralise. The association of Al with particles can be due to incorporation of Al into biogenic silica or scavenging of Al onto biogenic particles. The interaction between Al and biogenic particles leads to the coupled cycling of Al and silicate that is observed in some ocean regions. However, in other regions this coupling is not observed due to (i) advective processes bringing in older water masses that are depleted in Al, (ii) unfavourable scavenging conditions in the water column, (iii) low surface concentrations of Al or (iv) additional Al sources, notably sediment resuspension.

1. Introduction

Aluminium (Al) is one of the most abundant chemical elements on the planet. The average crustal abundance of Al is ~8.23 % by weight, three times less than the 28.15 % silicon (Si) in the earth crust. Both elements Al and Si are key constituents of clay minerals and clays are major sedimentary components on land and at the seafloor.

In the oceans the concentration of dissolved Al in seawater ranges from extremely low 0.1-0.5 nM in remote Antarctic Ocean subsurface waters (Middag et al., 2011b; Middag et al., 2012), to 174 nM in the deep waters of the (East) Mediterranean Sea (Chou and Wollast, 1997; Hydes et al., 1988; Rolison et al., submitted; this issue). In comparison, the concentration of dissolved silicate ranges from <0.1 µM in the surface waters of oligotrophic gyres in the central temperate oceans, to as high as ~30 µM in the deep North Atlantic Ocean and even ~180 µM in the oldest deep waters of the North Pacific Ocean (Sarmiento and Gruber, 2006). Silicon is a bio-essential nutrient for diatoms, which comprise ~40% of ocean phytoplankton productivity (Roberts et al., 2007). Diatoms utilize dissolved silicate, mostly H_4SiO_4, for the construction of their external opaline (SiO_2) frustules. Contrarily, for Al there is no known biological function.

The GEOSECS programme in the 1970s has been very successful in the worldwide mapping of the distributions of the major nutrients silicate, nitrate and phosphate in the oceans (Bainbridge et al., 1981). In the southward flowing North Atlantic Deep Water (NADW) the moderate nutrient concentrations are slowly yet steadily increasing with the southward transport. However, they remain in distinct contrast with the very high nutrients in the northwards flowing Antarctic Intermediate Water (AAIW) and Antarctic Bottom Water (AABW). These classical nutrient distributions of the West Atlantic Ocean are now in all textbooks and well understood due to the combination of the Meridional Overturning Circulation (Van Aken, 2007; Worthington, 1976; Worthington, 1981) or 'Deep Ocean Conveyor Belt' (Broecker, 1991) with the biological cycle of uptake by plankton in surface waters and remineralisation in deep waters (Redfield et al., 1963).

In context of the International Polar Year (2007-2008) GEOTRACES campaign, strong correlations between dissolved Al and silicate were found in the 200-2000 m depth range in the Arctic Ocean (Middag et al., 2009). This ocean and the seas north of Iceland are the major source for the North Atlantic Deep Water (NADW) (Rudels et al., 2000). In contrast, no Al-Si relationship exists in the Southern Ocean where the Al concentrations are extremely low and the silicate concentrations very high (Middag et al., 2011b). We hypothesised that along the pathway of the southward flowing NADW somehow the Al-Si relationship becomes lost presumably due to steady net scavenging removal of Al from the NADW (Fig. 1).

The basin-scale (100-10000 km) observation of a relationship between Al and Si in some, but by no means all, of the ocean basins, does not necessarily provide insight in the underlying microscopic plankton scale mechanisms. Latter mechanisms can be threefold, as well as any combination thereof. Firstly, it has been shown a trace amount of Al can become incorporated 'intrinsically' in the siliceous (opal) frustules of living diatoms (Gehlen et al., 2002). Secondly, Al may become adsorbed on the outside of such opaline frustules (Li et al., 2013; Moran and Moore, 1988; Moran and Moore, 1992). Upon settling of dead diatoms debris and dissolution of the frustules, the intrinsic and/or adsorbed Al also becomes partly dissolved again. Thirdly, any of the relatively heavy diatom frustules that have become incorporated in aggregates of biogenic debris (marine snow) will by their "ballast effect" enhance the export of such marine snow to the deep ocean (Armstrong et al., 2001). Upon remineralisation this marine snow, any Al associated with it, will likely yield an overall Al-Si relationship in deep waters.

The campaign of four consecutive GEOTRACES cruises (2010-2012) in the West Atlantic Ocean offered the opportunity to unravel and elucidate the remarkable coupling and de-coupling of Al and Si in the Atlantic Ocean, and hence also validate the preceding hypothesis (Figure 1). This paper presents the distribution, sources and sinks of subsurface Al along the West Atlantic section and details how the cycling of Al and Si can appear both coupled and uncoupled depending on the region. The surface distribution of Al and its use as a tracer of atmospheric dust input has been described separately to assist the interpretation of the distribution of iron (Rijkenberg et al., 2014) and cobalt (Dulaquais et al., 2014).

2. Methods

Samples were collected along the GEOTRACES GA02 Atlantic Meridional section of the Netherlands that consisted of 4 cruises (Fig. 2). Samples were collected using an all-titanium ultraclean CTD sampling system for trace metals (De Baar et al., 2008) with a new type of samplers constructed from PVDF (Rijkenberg et al., submitted). A total of 60 depth profiles over the full water column were sampled, each comprising 24 sampling depths, resulting in 1439 samples for dissolved Al. Upon recovery, the complete CTD sampling system was immediately placed inside a clean room environment sampling container where the sub-samples for trace metal analysis were collected. The water was filtered from the PVDF samplers over a 0.2 μm filter cartridge (Sartobran-300, Sartorius) under pressure (1.5 atm) of (inline pre-filtered) nitrogen gas. Henceforth, when referring to 'dissolved Al', this is operationally defined and includes colloidal Al smaller than 0.2 μm. Sub-samples for dissolved Al were taken in cleaned (see (Middag et al., 2009) for cleaning procedure) LDPE sample bottles (125 mL) after five rinses with the sampled seawater. Samples for shipboard analysis were stored in a refrigerator (4°C) and analysed usually within 24 h after sampling but always within 36 h.

Analyses of dissolved Al were performed on board with the improved lumogallion fluorescence flow injection method of Brown and Bruland (2008) with some minor modifications (Middag et al., 2011b). The samples of the 5 stations of cruise 64PE358 were measured in a shore based laboratory with the same method.

Samples were acidified to 0.024 M HCl (Baseline® Hydrochloric Acid, Seastar Chemicals Inc.) which results in a pH of ~1.8. The system was calibrated using standard additions from a 5000 nM Al stock solution to filtered acidified seawater of low Al concentration that was collected in the sampling area. A five-point calibration line and blank determination were made every day. The resulting concentrations in nM were converted to nmol kg^{-1} based on the seawater density under lab circumstances. The blank was determined as the intercept of the signals of increasing pre-concentration times (30, 60, 120 and 240 seconds) of the calibration water and was 0.15 nM (SD=0.035 nM; n= 57). The value of 0.2 nM was the maximum allowed blank before starting a series of analyses. The limit of detection, defined as three times the standard deviation of the lowest concentration observed, was 0.05 nM. The flow injection system was cleaned every day by rinsing with a 0.5 M HCl solution. All samples were analysed in triplicate.

An internal reference sample was measured in triplicate every day. This was a sub-sample of a 25 L volume of filtered seawater that was taken at the beginning of cruise 64PE319 (also used during for 64PE319) and cruise 74JC057 (also used for 64PE358). The relative standard deviation (i.e. the precision) of the measurement of the internal reference sample that was analysed on different days in triplicate was 3.34% (64PE319 and 64PE321, n=40), 2.27% (74JC057, n= 17) and 3.77% (64PE358, n=5). The relative standard deviation on single days was on average 1.3% and the absolute values were 6.46 and 9.83 nM for the first two cruises and the last two cruises, respectively.

As external comparison GEOTRACES and SAFe cruise reference samples were analysed for Al (Table 1). Results of the reference samples are in good agreement with the May 2013 'consensus values' (Table 1). Moreover, the data obtained at the BATS cross-over station agrees very well with a previous GEOTRACES occupation in 2008 in context of the US GEOTRACES Intercalibration cruise as reported previously (Cutter and Bruland, 2012; their Figure 11), and no statistical difference was observed between the two data sets of the 2008 and 2010 BATS occupation (Middag et al., submitted). Both datasets were sampled and analysed completely independently by UCSC in 2008 and NIOZ in 2010, respectively, with all laboratory calibration standards also independent, and at time of analyses each analyst (Dr. M. Brown, UCSC; Dr. Middag, NIOZ) not aware of the other dataset. In summary, the agreement of the independent profiles of dissolved Al analysed by UCSC (2008) and NIOZ (2010, this work) at BATS as well as the accompanying reference sample values (Middag et al., submitted), confirms the accuracy of this data. The complete dataset presented in this paper was submitted to the GEOTRACES Standards and Intercalibration committee who indeed deemed the data accurate and hence the dataset is included in the international GEOTRACES Intermediate Data Product ((The GEOTRACES group, submitted) http://www.bodc.ac.uk/geotraces/data/idp2014/). Regrettably, during the next occupation at the BATS site in context of the US 2011 zonal section cruise, the dissolved Al reported at BATS (Measures et al., in press) is too high (by ~22%) and also lacks supporting data of the international reference samples (for details see Electronic Supplement). Subsequently, this data has been excluded from the international GEOTRACES Intermediate Data Product.

The salinity (conductivity), temperature and depth (pressure) were measured with a CTD (Seabird SBE 911+). The CTD was calibrated before and after the expedition by the manufacturer (Seabird Electronics). Moreover, the conductivity sensors and oxygen sensors were calibrated against discrete water samples, analysed on board. Samples for nutrients were unfiltered and collected from the PVDF samplers in High Density Poly Ethylene (HDPE) sample bottles which were rinsed three times with sample water. Samples were stored in the dark at 4°C and analysed within 24 hours. Major nutrients nitrate (NO_3), nitrite (NO_2), phosphate (PO_4) and silicate ($Si(OH)_4$, from here on Si) were determined colourimetrical (Grasshoff et al., 1983) on a Bran en Luebbe trAAcs 800 Auto-analyser. The colourimetric method for Si measures the dissolved, monomeric orthosilicic acid ($Si(OH)_4$) and does not measure the polymeric, particulate or colloidal forms of Si. Thus the mentioned dissolved silicate concentration is the same as the dissolved concentration of (monomeric) elemental Si in seawater. A sterilised natural Reference Nutrient Sample (Kanso, Lot code AX) containing a known concentration of silicate, phosphate, nitrate and nitrite in Pacific Ocean water, was analysed in triplicate every run. The precision of this reference sample was typically around 0.6 % of the average value for silicate, phosphate, nitrate and around 3 % for nitrite. There was no significant difference between the shipboard measured values of Kanso and the consensus values. Additionally, the deepest sample analysed of a station of 24 samples, was kept and re-analysed within the next run of the next station of 24 samples as verification for variability between runs.

3. Hydrography

The Meridional Overturning Circulation, which ventilates the deep ocean is driven by deep water formation at high latitudes and upwelling in the remainder of the ocean (Van Aken, 2007). The Atlantic Ocean plays a crucial role in this overturning with the formation (in its northern extremities) and transport of NADW. Deep water formation and subsequent export at the high

northern latitudes leads to advection of warm low latitude water via the North Brazil Current and the Gulfstream. At the high southern latitudes, deep water formation in the Weddell Sea contributes to the formation of northward flowing AABW. Near the Antarctic Polar Front, another northward flowing water mass, the Antarctic Intermediate Water, is formed.

Several major water masses can be distinguished in the Atlantic Ocean (Fig. 3 and Table 2). In the northernmost part of the transect the upper waters are within the wind driven Subarctic Gyre, a cyclonic, in the Northern Hemisphere counter-clockwise, gyre in the subarctic and arctic North Atlantic. Deep water formation mainly takes place in the Labrador Sea and north of the Greenland-Scotland Ridge in the Greenland Sea and Arctic Basins. Deep water from the Labrador Sea flows directly into the North Atlantic Ocean as Labrador Sea Water (LSW). Deep water formed farther north needs to pass either the Denmark Strait between Iceland and Greenland and is known as Denmark Strait Overflow Water (DSOW), or enters the North Atlantic between Iceland and Scotland and is then known as Iceland-Scotland Overflow Water (ISOW). The ISOW flows to the western Atlantic Basin through the Charlie-Gibbs Fracture Zone (a deep sill in the Mid-Atlantic Ridge (MAR)) south of Iceland and is then also referred to as North East Atlantic Deep Water. In this paper we will refer to this water mass as ISOW to differentiate it from the generic North Atlantic Deep Water (NADW). The LSW, ISOW, and DSOW all contribute to the formation of the NADW that flows to the south and after mutual mixing over large distances still can be recognized from their particular characteristic properties. Therefore the NADW can be divided in upper, middle and lower NADW (uNADW, mNADW, and lNADW, respectively), which originate from LSW, ISOW, and DSOW, respectively.

Around the Grand Banks (~45 °N) the transition to the warmer surface North Atlantic Central Water (NACW) of the North Atlantic Gyre, an anti-cyclonic subtropical gyre, is encountered. This marks the northwestern corner of the Gulfstream system. Below the surface mixed layer, North Atlantic Subtropical Mode Water can be observed below the seasonal thermocline. The NADW is found between approximately 1200 and 4200 m, and can be well recognized by its relatively homogeneous high salinity core (S > 34.9, Fig. 3a) and relatively low nutrients (Fig. 3b and 3c). In the deep, below the NADW, the most northerly Antarctic Bottom Water (AABW) is observed. This water mass is formed by deep water formation around Antarctica in the Weddell and Ross Seas and flows north along the bottom as a cold, dense, Si-rich and Al-poor water layer (Fig. 3d and 3e). In the North Atlantic the AABW is also referred to as Lower Deep Water as it is not 'true' AABW anymore due to mixing during the northward advection. However, in this paper we will refer to it as AABW to emphasize the Antarctic origin.

Antarctic Intermediate water (AAIW) and the Upper Circumpolar Deep Water (uCDW) flow northward between the Atlantic Central Water in the main thermocline and the southward flowing NADW. The AAIW can be recognized at the southern end of our section by a subsurface salinity minimum, oxygen maximum, and elevated concentrations of Si. The uCDW can be recognized by an oxygen and temperature minimum as well as elevated nutrients (Stramma and England, 1999). Additionally, Subantarctic Mode Water can be distinguished, but for simplification this is regarded as part of the AAIW in this paper. Subtropical Mode Water (STMW) is formed during winter by convective mixing and both Northern and Southern Hemisphere varieties were encountered along the transect just below the seasonal thermocline.

An oxygen minimum zone (OMZ) is located between ~20°N and ~15°S at depths between ~ 100 and 1000 m (Fig. 3f). The OMZ is likely the result of local primary production in combination with decay and, in the Northern Hemisphere, by westward transport of low oxygen water along the North Equatorial Counter Current from the strong OMZ near the Cape Verde Islands of the coast of West Africa (Rijkenberg et al., 2014). Similar, in the Southern

Hemisphere there is westward advection of low oxygen water from the strong OMZ off the coast of Namibia.

4. Results and Discussion

The concentration of dissolved Al ([Al]) in the West Atlantic Ocean clearly reflects the distribution of the major water masses with high [Al] in the NADW of Arctic origin and low [Al] in the water masses of Antarctic origin (Fig. 3a). This Al distribution is the inverse image of the major nutrients nitrate and silicate (Fig. 3b and Fig. 3c), a clear testimony to its scavenged type behaviour (Bruland et al., 2014). The water masses of Antarctic origin (AAIW, uCDW and AABW) are characterized by low [Al] and high nutrient concentrations and are as such clearly distinguishable from NADW with high [Al] and relatively low nutrient concentrations. Antarctic waters are known for their high nutrient and low [Al] (e.g. Middag et al., 2011b; Van Beusekom et al., 1997) and keep that signature during northward advection into the Atlantic Ocean. Previously we hypothesized (Middag et al., 2011b) that the NADW, while flowing southwards in the West Atlantic basin, steadily accumulates more Si due to dissolution of settling diatoms debris, whereas Al is being lost due to continuous adsorptive scavenging removal that 'outcompetes' input due to remineralisation (Fig. 1). The silicon regeneration is not very well constrained. Data on particles in the deep Atlantic reported by Lam et al. (in press) (Lam et al., in press) suggest that opal is a small fraction of particles present in the subtropical gyre of the North Atlantic (mean of 3%). Indeed, Honjo et al. (2008) (Honjo et al., 2008) showed that the biogenic silica flux at 2 km depth is quite small in the central Atlantic (8-39 mmol m^{-2} yr^{-1}), but higher at low and high latitudes (up to 133 mmol m^{-2} yr^{-1} in the north Atlantic and 52 mmol m^{-2} yr^{-1} in the equatorial Atlantic).

Nelson et al., 1995 (Nelson et al., 1995) estimated diatoms to be responsible for 25-30% of primary production in the Sargasso Sea and that in the deep Atlantic 11.3 teramol of biogenic Si dissolves per year, the far majority of it in the water column, with only about 3% of the biogenic Si being buried. Recently, Treguer and La Roche (2013) estimated that ~25% of the exported Si remineralises in the water column whereas most of the remainder dissolves at the sediment water interface (with finally 3% burial). Our data indicates Si remineralisation in the water column as [Si] increases at constant salinity (Fig 3b) or neutral density (γ^n, Fig. 3e) within the NADW or based on mixing lines (see section 4.2). However, for both [Al] and [Si] there is diapycnal mixing evident along this long ocean section. The NADW [Al] maximum is diminishing and found at lower density in the southern part of the transect than in the northern part and similarly, the AABW [Si] maximum is diminishing and found at lower density during advection northwards (Fig. 3d and 3e). Based on our observations alone a qualitative estimate of Si regeneration is not feasible, nor is it the goal of this paper that aims to unravel the drivers of the oceanic dissolved Al cycle.

4.1 Aluminium and Silicate, inverse image or close resemblance?

4.1.1 Aluminium-Silicate relationship in the Subarctic Gyre

In the Subarctic Gyre, the [Al] and [Si] are positively correlated (rather than inversed) with both very low concentrations near the surface and an increase with depth. Using salinity, here the three components of what becomes NADW farther south can be distinguished (LSW, ISOW and DSOW, Fig. 4). The [Al] and [Si] show a strong positive correlation in the LSW and ISOW (Fig. 5a), but not in DSOW due to a sediment resuspension Al source (see section 4.3). The relationship [Al]/(nmol kg^{-1}) = 2.4 [Si]/(μmol kg^{-1}) – 15.1 (R^2=0.94 with p<0.001 for n=173

datapoints) of Al and Si is not due to simple conservative mixing of water masses as neither [Al] nor [Si] is correlated with salinity (Fig. 5b). The maximum in [Al] and [Si] around a salinity of ~34.92 is related to ISOW (see section 4.3.2 and Table 2). Correlations do appear when plotting [Al] or [Si] versus the potential temperature (θ) but there is far more scatter than in the [Al]-[Si] relations and the [Al]- θ and [Si]- θ correlations are not as strong ($R^2 \approx 0.6$; not shown). Nevertheless, these negative correlations of [Al] and [Si] with θ mainly reflect their common downward increase. This indicates that while mixing is of importance, there must be another process behind the strong Al-Si correlation. If Al and Si are released from remineralising particles, their concentrations should not only increase in unison downwards through the water column, but also during advection of water masses as particles sink into the advecting water mass from above. Indeed, when assessing data along lines of constant neutral density, [Al] and [Si] are positively correlated (Fig. 5c) at all γ^n intervals of 0.01 kg m^{-3}. Contrarily, along the same γ^n intervals, the weaker relations of [Al] with salinity and potential temperature as well as those of [Si] with salinity and potential temperature, change from positive to negative downward through the water column (Table 3). This supports the idea of Al and Si addition during advection of the water southwards that is unrelated to conservative mixing, and hence most likely due to release from settling biogenic particles.

4.1.2 Cycling of Al and Si connected via biogenic silica

The major external source of dissolved Al to the surface of the remote open ocean is atmospheric dust input (Maring and Duce, 1987). The main scavenger of Al was suggested to be biogenic diatom opal (Li et al., 2013; Moran and Moore, 1988; Moran and Moore, 1992). Additionally, biogenic diatom opal is due to its 'ballast effect' (~two times density of seawater) a key actor for the settling of miscellaneous biogenic debris into the deep ocean. As biogenic opal by this ballast effect aids in the export of organic carbon, the diatom opal flux is relatively more important for carbon export to the deep ocean compared to other particulate biogenic matter, even though diatoms contribute only ~40% to the primary organic carbon production in the surface waters of the ocean (Roberts et al., 2007). Consequently, sinking biogenic opal is the major carrier for bringing Al into the deepsea, be it either (i) truly within the opal (Gehlen et al., 2002; Koning et al., 2007; Stoffyn, 1979) and/or (ii) preferentially scavenged to biogenic opal by surface adsorption (Li et al., 2013; Moran and Moore, 1988; Moran and Moore, 1992) and/or (iii) scavenged onto biogenic particles (Hydes, 1979; Moran and Moore, 1988; Orians and Bruland, 1985) that are 'weighted down' by biogenic opal. However, please note that in the Atlantic Ocean calcium carbonate is dominant over biogenic opal (Honjo et al., 2008; Lam et al., in press), and likely dominant as ballast as well. If, despite the indications from previous studies, there is no strong preferential scavenging of Al onto biogenic opal, this implies that the connection between Al and Si might not be a direct causal relation, but related to their common transporter (biogenic particles where the opal or the calcium carbonate serves as ballast). Within the deep ocean the biogenic particles (partly) dissolve again, the Si (and other nutrients) remains dissolved but the released Al may rapidly become scavenged again by adsorption on other biogenic debris particles (or the remaining parts of the particle it was released from) (Fig. 1). In contrast to oxidative scavenging such as for manganese, where scavenged manganese oxides are largely insoluble (Sunda and Huntsman, 1988), Al is relatively soluble in seawater. In the absence of advective processes, an increasing Al concentration with depth below the surface is found if the scavenging intensity in the deep water is sufficiently low, as confirmed by a reversible scavenging model (Van Hulten et al., 2013). This increase with depth can be contributed to the remineralisation of the particles that contain the Al, or to the decreasing scavenging intensity that favours desorption

of Al, assuming the scavenging is a reversible process. Since remineralisation and desorption are difficult to differentiate as a source of Al, the term 'release' will be used as a generic term encompassing both dissolution and desorption.

The slope of the correlation between [Al] and [Si] (Fig. 5a) is similar to previous observations in the Arctic Ocean (Middag et al., 2009). As suggested in the Arctic Ocean, release of Al and Si from remineralising biogenic particles might explain the observed relationship between Al and Si. The slope of $\sim 2 \cdot 10^{-3}$ of the Al-Si relation in the subsurface waters of the Subarctic Gyre and Arctic Ocean (Middag et al., 2009) is in line with literature values for the Al:Si ratio of diatom frustules (Gehlen et al., 2002; Koning et al., 2007). This is consistent with the concept of diatoms in the surface waters accumulating 1 Al atom for every 500 Si atoms in their opaline frustules. Upon export of diatom particles into underlying subsurface waters, the siliceous diatom frustules are assumed to (partly) dissolve, releasing the same Al/Si ratio, which is resembled in the dissolved $\Delta Al/\Delta Si$ trend line of these subsurface waters. However, adsorptive scavenging of Al onto the outside of the diatom frustules followed by remineralisation would also correlate released Al with the released Si, thus based on the observations here we cannot distinguish between the two processes. Scavenging of Al onto biogenic particles in general followed by remineralisation would likely also correlate released Al with released Si if the particles associated with Al dissolve at roughly the same depths as the biogenic opal. Additionally, other studies found no biological incorporation of Al in frustules (e.g. Vrieling et al., 1999), thus whether diatoms are responsible for the observed Al-Si relationship remains unclear. However, given that Al is a particle-reactive element (Moran and Moore, 1992), it is inherently linked to the biological cycle due to scavenging on biological particles. Preferential scavenging onto biogenic opal has been observed (Li et al., 2013; Moran and Moore, 1988; Moran and Moore, 1992), but scavenging on any biogenic particle leads to export from the surface layer and partial release at depth if the biogenic particles remineralise.

4.1.3. The Al:Si relation is by no means a worldwide observation

Positive Al-Si relationships have thus far only been observed in specific ocean regions like the Arctic Ocean (Middag et al., 2009), the Mediterranean Sea (Chou and Wollast, 1997; Hydes et al., 1988; Rolison et al., submitted; this issue) and the North Atlantic Subarctic Gyre (this study). The confinement of the positive Al-Si relationship is due to the particle-reactive nature of Al (residence time 100-150 years (Orians and Bruland, 1985) versus 'inert' silicate (residence time >10000 years (Sarmiento and Gruber, 2006; Treguer and De La Rocha, 2013)) that causes a net removal of Al from deep waters while dissolved silicate is left behind in deep waters, uncoupling the Al-Si relation in the deep ocean. Therefore the positive Al-Si relationships are restricted to regions without significant inflow of 'old' water that is depleted in Al and enriched in Si. Additionally, in regions with low [Al] in surface waters, such as the Southern Ocean (Middag et al., 2009) or the Pacific Ocean (Orians and Bruland, 1985; Orians and Bruland, 1988), the uptake ratio Al:Si into opal of diatoms is deemed to be much lower (Collier and Edmond, 1984). Similarly, the Al association with diatoms by adsorption would, at low ambient [Al], yield lower Al:Si of the diatom particles (Van Hulten et al., 2013). As a result of the decoupling with age and the low surface [Al], no strong relationship between Al and Si is observed in the Southern Ocean (Middag et al., 2011b) and the Pacific Ocean (Orians and Bruland, 1985). Additionally, we postulate the scavenging intensity has to be 'just right' according to the 'goldilocks' fairy tale analogy, akin to the Cu balancing act for Cu availability in surface waters (Bruland et al., 2014). If scavenging is too high, released Al will be rapidly scavenged again and the [Al] will not show a nutrient-type profile. A very low scavenging intensity implies there are hardly any particles that

can serve as a source of both Al and Si, and any mutual increase with increasing depth will be (near-)impossible to detect. The Al-Si relationship can also be influenced by additional Al input like sediment resuspension or very high input of atmospheric dust deposition(Middag et al., 2011b) that serve as a significant source of Al, but not Si (see section 4.3. and 4.4).

4.1.4 Southwards Collapse of the Al:Si relationship

From ~40°N southward to ~30°S the NADW is slowly but steadily diminishing in thickness due to mixing with overlying and underlying water masses (Fig. 4). At 40°N, NADW extends between 1500m and 4000m depth to end up between 2000m and 3000m depth at 30°S. Within this NADW there is a significant (p<0.001) positive correlation between [Al] and [Si], but there is quite some scatter. When divided in four latitude zones, one finds significant correlations (p<0.001) between [Al] and [Si] with better fits for which the slope ΔAl/ΔSi decreases steadily from north to south (Fig. 6). This systematic decrease of the slope of regression may be due to a steady increase of [Si] due to deep dissolution of vertical settling diatom debris in combination with a steady decrease of [Al] due to its continued net deep water scavenging (Fig. 1, and see section 4.2). Additionally, the Al:Si ratio of the diatoms in surface waters is likely to be lower in the Southern Hemisphere than in the Northern Hemisphere, as result of lower ambient [Al] in surface waters of the Southern Hemisphere (Fig. 3a).

In the equatorial region, at individual stations, the oxygen minimum corresponds with an [Al] maximum (Fig. 7a) and [Al] shows a significant negative correlation with the oxygen concentration (R^2=94, n=29, p<0.001), as well as a significant positive correlation with the apparent oxygen utilisation (AOU) (Fig. 7b). The OMZ, in general does not appear as an [Al] maximum in the colour scale figures as observed for iron (Rijkenberg et al., 2014). However, the deepest parts of the OMZ correspond to the upper limit of the Al-poor AAIW that advects from the south (Fig 3d and 3f). Additionally, the OMZ/AAIW/uCDW depth interval is overlain and underlain by Al-rich waters, the dust influenced surface waters and Al-rich NADW, respectively, giving the appearance of an Al minimum. Despite this overall Al minimum in the OMZ/AAIW and uCDW as observed in the colour scale figures (Fig 3a), the vertical profiles clearly show a small Al maximum corresponding with the oxygen minimum. Additionally, within the centre of the OMZ (AOU > 150 µmol kg^{-1}) , [Al] is negatively correlated with the oxygen concentration, indicating a release of Al associated with remineralisation. In the Southern Hemisphere, however, there is no overall relationship between [Al] and AOU for the entire OMZ, but several individual stations in the OMZ region do show strong regressions (R^2 up to 0.98; Supplementary Table S1). This weaker overall relation might be due to the stronger influence of AAIW in the Southern Hemisphere, but the lower sampling resolution or different season of sampling cannot be excluded either. Similar to the western Atlantic, Measures et al. (in press) observed an Al minimum in the eastern Atlantic that corresponded to the OMZ and AAIW. However, they did not note the presence of a small [Al] maximum in the vertical profiles, implying there might be regional or seasonal differences in the amount of Al release and/or the balance between Al release and (re-)scavenging in OMZs. Interestingly, inspecting the vertical profiles reported by Measures et al. (in press) as published on the webpage of the funding body data management office (Measures, 2013), does reveal small [Al] maxima around the depth of the oxygen minimum, after all indicting there might in fact be Al release from remineralising particles in the eastern Atlantic as well. However further study of latter features is deemed outside the scope of the current study of the West Atlantic Ocean.

For dissolved iron, Rijkenberg et al. (2014) estimated uptake of iron with respect to carbon (C) uptake in the surface layer based on the observed relationship with AOU. Similarly, for the

Northern Hemisphere OMZ (AOU > 150 μmol kg^{-1}, 200-800m depth) between 10°N and the equator, we now find a significant relationship [A]/(nmol kg^{-1}) = 0.06AOU/(μmol kg^{-1}) - 3.62 (R^2=0.78, n=29, p<0.001). Using the same assumption as Rijkenberg et al. (2014) of for the C:AOU ratio of 1.39, results in an Al:C ratio of 4.3 x 10^{-5} (mol Al per mol C) for the apparent net mineralization/dissolution of both Al and C within this OMZ.

Next by assuming an Si:C ratio 1:7 in diatoms (Brzezinski, 1985), and diatoms being responsible for ~40% of primary production and export (Roberts et al., 2007) would give an Al:Si in the order of 0.8 x 10^{-3} derived for the OMZ. This estimate remains largely speculative due to the errors associated with the underlying assumptions and, in addition, preferential preservation of biogenic silica (Nelson et al., 2002), as well as any is re-scavenging of Al by the particle rain from the productive OMZ source waters have not been taken into consideration. Nevertheless, the estimate is in the range of values observed for the slope of regression (ΔAl/ΔSi) found for the Subarctic Gyre (Figure 5a) and the other latitude regions of the NADW (Figure 6). Please be reminded that these various basin-scale Al/Si relationships thus far do not provide specification on the underlying microscopic mechanism(s). However, the relationship between Al and oxygen in the OMZ is a strong indicator for Al release during particle remineralisation.

4.2 Scavenging loss

When plotting θ versus S for the deep and intermediate waters south of 40° N (i.e. south of the Subarctic Gyre) where AABW is the deepest water mass, clear continuous mixing lines become apparent (Fig. 8a). Relatively salty and warm uNADW mixes with mNADW and lNADW that are both colder and less saline. Deeper, lNADW mixes with the cold and relatively fresh AABW, visible in the change in direction of the mixing line around θ = 1.8°C, S = 34.88. In the southernmost part of the transect (Fig. 8a) most of the NADW has disappeared and a different mixing line appears; mixing of the cold and relatively fresh bottom waters with a mixture of lower and upperCDW (labelled as uCDW in this paper). Similar mixing lines show when plotting [Si] versus salinity (Fig. 8b). The different water masses show more clearly when plotting [Al] versus salinity (Fig. 8c). The [Al] is not a water mass characteristic, but if it behaves conservatively, it should plot as a mixing line versus salinity when two water masses mix, i.e. if only mixing is of importance this results in a straight line. A source or a sink during mixing of two water masses leads to convexity and concavity, respectively.

The uNADW has a relatively low [Al] and high salinity and mixes with mNADW and lNADW that has highest [Al] and lower salinity. Further down the water column (salinity ≈ 34.88) there is a change in the direction of the mixing line as Al-rich lNADW mixes with lower-salinity and Al-poor bottom water with Antarctic influence. In the southernmost part, again the mixing of bottom waters with CDW results in a different mixing line. The mixing line between NADW and AABW shows concavity whereas this does not show in the [Si]-salinity or θ-salinity diagram, this concavity a clear indication of loss of Al along the mixing line. However, mixing with another (i.e. third) relatively [Al]-poor end member could be an alternative cause of the concavity. Between ~10°S and 35°S, there are some anomalous data points in the property-property plots around a salinity of 34.9 at depths between 2500 and 3500 m in the transition between NADW and AABW, most notable in the [Al]-S diagram (Fig. 8c; green and blue data points). These points have lower [Al] than would be expected based on the salinity and slightly higher [Si] and θ. The higher θ rules out influence from the underlying Al-poor AABW or overlying Al-poor uCDW/AAIW. These observations appear inconsistent with a different low [Al] end member as a cause for the observed concavity in the [Al]-salinity mixing lines between

lNADW and AABW in the deep basin. Therefore, this concave shape strongly indicates scavenging loss of Al in the deep basin. This is further confirmed by plotting [Al] versus neutral density (Fig. 8d) that shows lower [Al] at equal neutral density in the southern parts of the transect compared to the northern parts. Overall, [Al] in the near bottom water in the West Atlantic increases in a northward direction due to mixing with the overlying Al-rich NADW.

Indications for scavenging of Al within the NADW during its southward advection are visible in the decreasing Al/Si ratio in NADW in the southward direction. However, using this approach it is not possible to distinguish between the effects of Al scavenging versus mixing with the under- and overlying water masses (AAIW/uCDW and AABW) with low [Al] and high [Si]. Alternatively, within the NADW in the salinity range above 34.9, [Al] is lower at more southern stations for a given salinity (Fig. 8c) or neutral density (Fig. 3d and Fig. 8d). Contrarily, above a salinity of 34.9, θ and [Si] fall along the mixing line and, if at all, southern stations appear to be on the higher end (Fig. 8a, Fig. 8b and Fig. 3e). This rules out mixing with underlying cold, Si-rich AABW as a cause of lower [Al] further southwards, as well as mixing with the warmer, relatively Si-poor overlying iNADW/uNADW. Thus in the NADW there appears to be a sink of Al, confirming scavenging during the southward advection of NADW as suggested based on the Al-Si relationship (Fig. 6). Addition of Al due to remineralisation most likely plays a role as well (Fig. 5 and Fig. 7), but on the basin-wide scale, scavenging is the dominant process (Fig. 6 and Fig. 8c). The net amount of scavenging cannot be determined based on mixing lines as it requires detailed information on the [Al] concentrations of the various water masses that are mixing. Given the additional sources of Al in the ocean such as sediment resuspension (see section 4.3 Sediment resuspension sources) and subduction of Al-rich water masses (see section 4.4.1 and 4.4.3) that are still poorly constrained, this needs further research and the scavenging of Al can currently only be established qualitatively.

The net scavenging of dissolved Al in NADW now shows clearly from this long meridional section, whereas it was not observed in a previous east west transect (Measures and Edmond, 1990). The here demonstrated net scavenging loss as well as the likely biologically mediated cycling implies that the use of Al as a tracer of water masses is limited to its use as a merely qualitative tracer due to its non-conservative nature.

4.3 Sediment resuspension sources

4.3.1 North Atlantic Deep Water

Surface waters in the Subarctic Gyre have low [Al], [Si] as well as [NO$_3$] (Fig. 3). This is also the case for the surface waters north of Iceland that are the source waters for the deep water formation that results in NADW (e.g. Dickson and Brown, 1994; Middag et al., 2009; Van Aken, 2007). The NADW, however, has elevated [Al] (Fig. 3a). Apparently the signature of low [Al] is lost during formation (sinking) and advection of NADW into the Atlantic Ocean, unlike the Antarctic counterparts (AABW, AAIW and uCDW) that retain their low [Al] far into the Atlantic. There are two hypothesis to explain the elevated [Al] in NADW; (i) atmospherically deposited Al that is removed from the surface waters to the sediment-water interface where remobilisation of Al occurs (Hall and Measures, 1998), (ii) sediment resuspension (Moran and Moore, 1991). These hypotheses share that the [Al] builds up after the initial sinking of the surface waters that eventually form NADW.

4.3.1.1 Hypothesis 1

The hypothesis of Hall and Measures (1998), was based on their observations in the East Atlantic. The higher dust deposition in the Atlantic than in the Pacific or Southern Ocean would explain the higher deep water [Al] in the Atlantic. The basin-wide diffusive type profile (increasing concentrations towards the seafloor) they observed in the deep waters of the eastern North Atlantic Ocean supported this hypothesis. However, it has now become clear that most of the West Atlantic does not have a diffusive type profile, but rather has decreasing concentrations towards the seafloor due to the presence of Al-poor AABW. Thus the basin-wide flux they calculated for the deep Atlantic from the sediments cannot be used to explain the elevated NADW values. In the West Atlantic, interaction with the near-bottom water mass in general constitutes a loss of Al for the NADW instead of a source (Fig. 8c) disproving the hypothesis that atmospheric dust deposited to the seafloor is the source for the Al-rich NADW.

4.3.1.2 Hypothesis 2

The DSOW starts out with low [Si] and intermediate [Al] in the far north but then becomes strongly enriched in Al and somewhat in Si as DSOW cascades downslope over the seafloor. There is a strong increase of [Al] towards the seafloor in the DSOW and near bottom [Al] increases linearly with decreasing latitude towards a distinct [Al] maximum at ~45°N (Fig. 9). Around this latitude, the DSOW loses contact with the seafloor as it becomes underlain by northward flowing AABW that is low in [Al] but high in [Si] (Fig. 3a and Fig. 3b). Elevated [Si] in bottom waters has been postulated to prevent release of Al from aluminosilicates in sediments (Mackin and Aller, 1986 (their equation (3) and related text); Van Hulten et al., 2014). Conversely, the low [Si] in the DSOW favours release and accumulation of [Al] in bottom water DSOW. Additionally, the well-known fast flow rates of DSOW and related intensive bottom nepheloid layer of re-suspended sediment particles (Biscaye and Eittreim, 1977)(Fig. 10), enhances the contact exposure of sediment particles with seawater thus enhancing the overall rate of Al release. The linear increase of [Al] downstream in the southward flowing DSOW (Fig. 9) in the absence of any other Al source, agrees with the hypothesis by Moran and Moore (1991). Sediment resuspension associated with nepheloid layers along the western boundary of the North Atlantic, like around the Grand Banks, is a source of dissolved Al. Moran and Moore (1991) also conducted sediment resuspension experiments, which indeed demonstrated an increase in dissolved Al by adding natural suspended sediments to seawater. Hall and Measures (1998), on the other hand argued, that a lateral gradient in deep water [Al] between the eastern and western basins should exist due to the less turbulent bottom flow in the eastern basin. From the data available to Hall and Measures (1998), such a gradient was not apparent. However, currently much more data is available for the West Atlantic to make a good comparison. Briefly, Hall and Measures (1998) reported [Al] of ~10-14 nmol kg^{-1} (highest values in the water column) around 3000 m depth in the eastern basin at 56°N 25.5°W. At similar latitude (3 stations between 54°N and 57°N) in the western basin we now observe much higher values around 20 nmol kg^{-1} around 3000 m depth and even higher values up to 25 nmol kg^{-1} near the seafloor (Fig. 3). Moreover, [Al] up to 35 nmol kg^{-1} as observed in the deep north western basin (Fig. 3) is, to the best of our knowledge, higher than any value ever reported in the deep northwest basin. Thus it is now shown that the energetic bottom flow of the DSOW in the West Atlantic leads to elevated [Al], whereas the relatively stagnant bottom waters in the northeast basin have lower concentrations (Hall and Measures, 1998). The sediment resuspension source for Al is also confirmed in an ocean general circulation model that includes biogeochemistry and Al cycling (Van Hulten et al., 2014) and now also confirmed for the northwestern Atlantic basin by Measures et al. (in press).

The highest beam attenuation coefficient (indicator of sediment resuspension; Fig. 10) is around 40°N, whereas the highest [Al] is observed north of that. However, around 40°N influence of Al-poor AABW (based on θ and [Si] (Fig. 3b)) is observed and the elevation caused by sediment resuspension is thus an addition to the lower initial [Al] of AABW. Indeed in bottom water with a clear AABW influence, the highest [Al] is observed in the region around 40°N with sediment resuspension.

4.3.2 Subarctic Gyre

The two deepest components of NADW, namely ISOW and DSOW, have similar origins but different advection routes (e.g. (Dickson and Brown, 1994)). Therefore, differences in [Al] in the different water masses are likely related to mixing and other processes along the advection routes. The ISOW is formed by mixing of water that overflows the shallow sills between Iceland and Scotland with the warm and salty NACW, the latter estimated to constitute between 25 and 50% of ISOW observed in the Iceland basin (Van Aken and De Boer, 1995). In the Iceland basin, the ISOW mixes with the underlying AABW influenced water mass (Lower Deep Water), giving origin to the elevated [Si] levels observed in the ISOW compared to DSOW. North of 54°N in the north-western basin, ISOW has an Al maximum of ~17 nmol kg^{-1} coinciding with a [Si] maximum of ~13 μmol kg^{-1} at around 2500 m depth. The ISOW in the north-eastern basin has a previously reported [Al] between 10 to 14 nmol kg^{-1} and a [Si] between ~15 to 22 μmol kg^{-1}(Hall and Measures, 1998). The lower [Si] in the north-western basin indicates that ISOW here has been diluted with relatively [Si]-poor LSW or DSOW during the westward advection. Since both LSW and DSOW have lower or similar [Al] compared to ISOW in this region, this suggests a source of Al for ISOW, most likely interaction with the sediments when passing along and through the MAR. However, temporal variation or offsets between different data sets cannot be excluded either, so this remains speculative.

South of 54°N there still is a deep [Si] maximum related to the inflow of Si-rich ISOW and underlying relatively Si-poor DSOW. Contrarily, no [Al] maximum is observed in ISOW due to thelarge sediment resuspension source of Al in the underlying DSOW. The [Si] maximum sinks from 3000 to 4000 m depth and concentrations increase from 14 to 22 μmol kg^{-1} [Si] southwards between 54°N and 45°N. At 43 °N, there is no [Si] maximum in the deep water column anymore as concentrations of Si increase steeply in the near bottom water whereas [Al] decreases, clearly indicating the influence of AABW. Between 54°N and 45°N there might be some input of the relatively fresh (less saline) [Si]-rich AABW as there is a negative correlation (R = -0.90) between [Si] and salinity below the depth of the [Si] maximum. Contrarily, north of 54°N there is a positive correlation, due to the mixing with relatively fresh (less saline) [Si]-poor DSOW with ISOW. As [Al] does not decrease in the near bottom water between 54°N and 45°N where the [Si]-salinity distribution suggests there could be input of relatively Al-poor AABW, this agrees with sediment resuspension input of Al being the dominant process. From 43°N southwards, the influence of AABW is clearly dominant in the near-bottom layer as [Al] decreases towards the sediments, possibly due to hindering of further sediment dissolution by the high [Si] in AABW.

4.3.3 AntArctic Bottom Water

Around 40°S, a very modest sediment resuspension source of Al is observed in the near bottom AABW, leading to a small concentration increase of ~ 2 nmol kg^{-1} compared to depths shallower (~4500 m) and at the southernmost part of the transect (Fig 3a). The [Si]-salinity plot shows a straight mixing line with the highest [Si] associated with low salinity AABW as one would expect (Fig. 8b). However, the [Al]-salinity plot shows curvature with high [Al] in the

near bottom lowest salinity samples (Fig. 8c), implying a bottom [Al] source. This also shows in the vertical profiles and colour plot as an increase with increasing depth in near bottom waters south of 30°S (Fig. 3a). This is contrary to what is observed in the near bottom layer elsewhere along the transect where [Al] decreases towards the seafloor in the 'purest' near-bottom AABW. A sediment resuspension source is also supported by the elevated beam attenuation coefficient in the southernmost part of the transect (Fig. 10). North of 30°S, mixing between relatively Al-rich, Si-poor NADW and relatively Al-poor, Si-rich AABW becomes the dominant process and no bottom Al source is apparent (Fig. 8c). Additionally, scavenging of Al becomes apparent during the northward advection of AABW and the southward advection of NADW (Fig. 6 and 8; see also section 4.2).

4.4 Subtropical Mode Water and Antarctic Intermediate Water

4.4.1 Southern Hemisphere Subtropical Mode Water

In the southern part of the transect, there is a subsurface maximum in [Al] (about 5 nmol kg^{-1}) around 300-400 m depth, above the depth of the AAIW (Fig. 3a and Fig. 11). This maximum appears around 40°S and is not visible anymore from around 20°S northwards in the colour contour plot, although the maximum is still visible in the vertical profiles. The depth of the Al maximum deepens in a northward direction from about 300 to 400 m depth along the 26.55 neutral density isopycnal (Fig. 11), coinciding with STMW (STMW type 2 as defined by Provost et al. (1999)). This STMW is formed near the Brazilian continental shelf and subducts into the main thermocline and has been observed along the South American coast between 40 and 25 °S between 100 and 450 m depth (Provost et al., 1999; Stramma and England, 1999).The STMW is formed during winter, mainly in the south-western region of the South Atlantic Gyre in the Brazil Current overshoot (Provost et al., 1999). However, the [Al] observed in the source region of STMW along the current transect is lower than the concentrations of the subsurface maximum in the STMW. Since STMW is formed by deep winter mixing that mixes surface waters with the underlying waters down to depths of 200 - 400 m (Donners et al., 2005; Provost et al., 1999), this implies that either the surface [Al] is higher in winter during formation of the mode water or there must be an additional source of Al to the Southern Hemisphere STMW. Most dust deposition is believed to occur during the Northern Hemisphere summer (Gao et al., 2001) as the major sources of dust are located in the Northern Hemisphere. This is when the mode water in the South Atlantic is formed (Southern Hemisphere winter). However, if the dust were the only Al source, this would lead to lower rather than higher [Al] during mode water formation as the mixed layer is several times deeper than in summer, whereas only about 2 times more dust gets deposited (Gao et al., 2001). Alternatively, dust input from South America (Patagonia) might be important in the source region of STMW (Dammshaeuser et al., 2011; Deng et al., 2014), but it is unlikely that such high deposition occurs in the Southern Hemisphere winter (Gao et al., 2001).

Vink and Measures (2001) observed much higher [Al] in the Brazil current (May 1996) of > 20nM compared to ~5 nmol/kg in the same region for this study. This implies that [Al] in the southward flowing Brazil Current is quite variable, but inaccuracy of the previous data cannot be excluded either, as a large correction (up to 100% of the reported values) was applied to account for contamination issues. Variations in [Al] in the Brazil current could be related to variations in dust deposition closer to the equator and recirculation of low latitude water into the Brazil Current as well as the Benguela Current that feeds into the Brazil Current around 15°S (Stramma and England, 1999). At this latitude higher [Al] was also observed in surface water along the current transect (~12 nmol kg^{-1}). The Brazil Current feeds into the source region of the

subtropical mode water formation region (Provost et al., 1999) and mode water formation occurs during times of highest dust deposition near the equator. Assuming flow rates in the order of ~ 50 cm s^{-1} for the Brazil current (Stramma, 1989), this current has the potential to deliver elevated [Al] from the equatorial region to the STMW source region with a time lag of about 2-3 months. This has the potential to explain the higher [Al] observed in STMW at depth versus [Al] in STMW source surface waters in the Southern Hemisphere summer/fall. Alternatively, increased winter-time mixing and sediment resuspension over the South American continental shelf could be a source of [Al]. Subsequent transport of this [Al] offshore in the Falkland (Malvinas) Current – Brazil Current confluence zone into the STMW source region could be a feasible explanation for the elevated [Al] in STMW as well. Offshore transport in this confluence zone was also suggested based on the dissolved iron distribution (Rijkenberg et al., 2014).

4.4.2 Antarctic Intermediate Water

The source regions for AAIW in the western South Atlantic are mainly surface waters in the northern Drake Passage and in the Falkland (Malvinas) Current loop (Stramma and England, 1999). The uCDW that underlies AAIW feeds out of the Antarctic Circumpolar Current into the South Atlantic. Surface [Al] in the northern Drake Passage is around 0.5 nmol kg^{-1} except over the south American continental shelf where concentrations are elevated due to continental run off (Middag et al., 2012). The only data near the Falkland (Malvinas) Current loop from this study was on the southernmost station were a surface concentration of ~ 4 nmol kg^{-1} was observed. The [Al] in uCDW is around 0.5 nmol kg^{-1} in Drake Passage (Middag et al., 2012) and has similar values around 1 nmol kg^{-1} in the Antarctic circumpolar current along the zero meridian (Middag et al., 2011b). The AAIW and uCDW [Al] are around 1.5 nmol kg^{-1} in the southernmost part along the current transect and increase with advection northward (Fig. 3a and 3d). Based on [Al], AAIW and uCDW are indistinguishable, implying that the higher [Al] that presumably exists in the Falkland (Malvinas) Current loop (AAIW source region) does not have a noticeable impact on the [Al] in AAIW in the South Atlantic along the current transect. The increasing [Al] with advection northwards in AAIW and uCDW is mainly due to mixing with the underlying Al-rich NADW as well as the overlying Al-rich STMW (north of 40°S) and the Al-rich warm surface and subsurface waters near the equator. Additionally, some Al could also be added to the AAIW and uCDW during remineralisation of biogenic particles as observed in the oxygen minimum zones (Fig. 7). However, plotting [Al] versus salinity in the AAIW and uCDW (not shown) gives a linear relationship, implying mixing is the dominant factor explaining the increasing [Al].

4.4.3 Northern Hemisphere Subtropical Mode Water

As previously observed (Measures et al., 2008), there is Al-rich STMW in the northern Atlantic as well. Their observation of > 18 nmol kg^{-1} around 300 m depth between 35 and 20°N in the North East Atlantic is largely consistent with the current observations in the Northwest Atlantic (Fig. 11). However, the values observed in this more westerly transect are higher (up to ~30 nmol kg^{-1}) and a subsurface maximum is observed as far north as 54°N. The subsurface maximum appears shallower in the northern part of this transect, around 150-200 meter depth, and is located around 300 m southwards. This subsurface maximum remains distinguishable as far south as 20°N. The higher [Al] is consistent with the main volumetric contribution to the STMW of the Atlantic being from the region in the Sargasso Sea, north of Bermuda (Worthington, 1959). During the current transect, surface [Al] north of Bermuda was up to 31 nmol kg^{-1}, similar to the highest subsurface maxima in the same region and previously even higher concentrations (~35 nM) were observed in this region (Measures et al., 2008). As outlined

by Measures et al. (2008), atmospheric deposition in the source region of STMW is a likely source of the elevated [Al] observed in STMW (see also section 4.5). The subsurface Al maxima with relatively elevated salinity and temperature as far north as 54°N indicate that the STMW from the Gulfstream system penetrated into the boundary currents around the subarctic gyre, and is still recognizable there from its chemical signature.

4.5 Surface distribution

Surface [Al] is depleted at higher latitudes and extremely elevated at the lower latitudes, mainly between 10 and 30° N. This is largely consistent with the dust deposition distribution to the Atlantic Ocean as has been observed in previous studies (e.g. Kramer et al., 2004; Measures and Vink, 2000; Measures et al., 2008) as well as modelling studies (Han et al., 2008; Van Hulten et al., 2013; van Hulten et al., 2014). The Saharan desert is the largest source of dust to the Atlantic and the high [Al] north of the equator reflects this source (e.g. Measures et al., 2008) that is a source also for Fe and Mn (Rijkenberg et al., 2014). Since the surface [Al] reflects the atmospheric dust deposition, [Al] has been used to infer the amount of dust deposition to the ocean (initial model by (Measures and Brown, 1996)), although uncertainty about the residence time of Al might lead to over- or under-estimations (Dammshaeuser et al., 2011). The application of surface [Al] as an atmospheric dust tracer has been written up separately and surface Al-based dust fluxes were calculated (Dulaquais et al., 2014; Rijkenberg et al., 2014). The latitudinal position of the high [Al] around 20-30°N does not quite match with knowledge on maximum dust deposition closer to the equator (Mahowald et al., 2002; Van Hulten et al., 2013)), but does match with elevated concentrations of Fe and Mn (Rijkenberg et al., 2014). This implies that the dust deposition between 20-30°N has previously been underestimated, or that the dust deposited in this region is relatively soluble. It has been shown that the origin of dust, as well as atmospheric processing have a significant effect on the solubility (Baker et al., 2006; Baker and Croot, 2010). Alternatively, the scavenging intensity as well as the mixed layer depth in the deposition area also have a strong effect on the metal concentrations resulting from dust deposition (Dulaquais et al., 2014). More targeted research is needed to unravel the exact cause of the elevated [Al] in this region, but modelling studies hint at relatively low scavenging rates in these surface waters, and hence a longer surface water residence time of Al (Dulaquais et al., 2014; Han et al., 2008; Van Hulten et al., 2013). Regardless of the exact source of the elevated [Al] in this region, advection of water from this latitude with the Gulfstream likely plays a role in the elevated [Al] observed in the source region of Northern Hemisphere STMW (see section 4.4.3).

4.6 Basin wide comparisons

4.6.1 Atlantic Ocean

When comparing data from 40°N in the eastern basin (Middag, 2010) with data from the current transect at 40°N, the deep [Al] is similar. What is striking though is the difference in the shape of the depth profile. In the western basin the NADW is overlain and underlain by water with lower [Al], whereas in the eastern basin the NADW is overlain and underlain by water with higher [Al]. At 40°N along the current transect in the western basin, there is a clear [Al] minimum around 1250 m depth (mixture of LSW and remnants of AAIW and uCDW) overlaying the main NADW body, whereas in the eastern basin there is a striking Al maximum at 1000 m, coinciding with Mediterranean Outflow Water above the NADW with extremely elevated [Al] (e.g. (Measures, 1995; Measures et al., in press; Middag, 2010)). Below NADW, the Al profiles show a clear decrease in the AABW influenced water layer in the western basin, whereas this

decrease is absent in the eastern basin and values continue to increase until the seafloor. The mixing of NADW with overlying and underlying water with low [Al] versus high [Al] in the western and eastern basin, respectively, might be the reason for the absence of an obvious west to east gradient at lower latitude whereas such a gradient is now observed farther north (see section 4.3). Moreover, it was suggested (section 4.3) that the [Al] in ISOW increases when this water mass passes the MAR, suggesting the NADW might also pick up Al when it passes the ridge from the eastern to the western basin by sediment-water interaction. Something similar was observed in the Southern Ocean where deep [Al] also became elevated where water was passing around seafloor elevations like Maud Rise (Middag et al., 2011b), creating a more turbulent flow.

Previously no significant hydrothermal source of [Al] was reported (Elderfield and Schultz, 1996; Lunel et al., 1990; Middag et al., 2009; Middag et al., 2011b; Middag et al., 2012), but it was suggested that increased [Al] around the MAR might be the result of entrainment water enriched in Al by sediment resuspension on the flanks of mid ocean ridges, rather than originating from the vent fluid itself (Lunel et al., 1990). Recently, Measures et al. (in press) reported a similar Al enrichment as Lunel et al (1990) that indeed cannot be explained by known Al endmember concentrations for hydrothermal fluids and a sedimentary source appears most likely as also suggested here for waters traversing the MAR (see section 4.3). Along the meridional West-Atlantic section, elevated concentrations of manganese and iron from hydrothermal origin were observed (Rijkenberg et al., 2014), but for the same samples there was no effect distinguishable for the Al distribution. This implies a hydrothermal source for [Al] is minor on the basinwide scale. In line with this, Measures et al (in press) also only reported a very localised [Al] enrichment near the MAR in their zonal section. Nevertheless, Measures et al. (in press) still invoke a significant hydrothermal Al source for the eastern basin based on a mixing line fitted through three endmembers (based on [Al] and [Si]) as follows: (i), the hydrothermal plume with elevated [Al] in the West Atlantic at the neutral density of lNADW, (ii) the West Atlantic AABW with elevated [Si] and (iii) the bottom water mass observed on the eastern site of the MAR. However, the [Al] in the hydrothermal plume endmember of ~ 32 nmol L^{-1} is, after taking the ~22% overestimation into account, merely around ~24 nmol kg^{-1} (see section 2 and electronic supplement). The latter value is nearly identical to the ~23 nmol kg^{-1} [Al] observed around 12° N in lNADW along the current western basin meridional section with otherwise similar [Si] as used for the invoked hydrothermal endmember by Measures et al. (in press). The latter latitude of 12° N is the latitude of the Vema fracture zone, the principle connection between the West and East Atlantic basin (Measures et al., in press and references therein). Hydrothermal input of Al along our meridional section is highly unlikely as this meridional section kept further west than the region where Measures et al. (in press) observed hydrothermal input at two stations overlying, and directly adjacent, to the MAR. Additionally, along our meridional section, [Al] in lNADW is continuously decreasing during southward advection (Fig. 3a and 3d). Moreover, there is no elevated [Al] coinciding with the observed elevated iron and manganese from hydrothermal sources along this meridional section (Rijkenberg et al., 2014). Therefore mixing of water masses without hydrothermal input of Al can explain the observed Al distribution by Measures et al. (in press) equally well.

Measures et al. (in press) noted a hydrothermal source was not included in the initial model by Van Hulten et al. (2013) and question the validity of this assumption and the model. This assumption by Van Hulten et al. (2013) was based on extensive plumes of hydrothermal iron and manganese in the Artic and Antarctic that were not accompanied by elevated [Al] (Klunder et al., 2011; Klunder et al., 2012; Middag et al., 2009; Middag et al., 2011a; Middag et al., 2011b). The new observations of Measures et al. (in press) at the MAR, may just as well be attributed to

sediment resuspension (Lunel et al., 1990). Additionally, this very localised observation over the MAR has a negligible effect on the basin wide observations in the West Atlantic which were the focus of the model. It has now been demonstrated the assumption by Van Hulten et al. (2013) in fact is valid and reasonable for the general distribution of Al in the Atlantic. The initial model (Van Hulten et al., 2013) focussed on the main drivers of the oceanic Al distribution. In the updated model (van Hulten et al., 2014), a sediment resuspension source is included and thus indirectly incorporates mid ocean ridge region inputs as sediment resuspension. The latter appears the most likely source of the observed [Al] enrichment on the MAR in the zonal section (Lunel et al., 1990). However, future targeted research will need to establish the exact origin of [Al] enrichments over mid ocean ridges, but based on the currently available evidence these enrichments do not appear significant for the basin wide distribution of Al.

Measures et al. (in press) report no evidence for release of Al from biogenic (Si) particles. Their conclusion is based on their observations in the eastern OMZ, where there might be evidence for release after all (see section 4.1.4). Otherwise, the absence of net release might be related to more intense scavenging in this highly productive region (see section 4.1.4). The imprinting of the Al:Si signal onto the water column as observed in the subarctic gyre due to release from remineralising particles is not expected in the eastern OMZ where mixing between different water masses with a wide range of original [Al] and [Si] (i.e. Mediterranean Overflow Water, AAIW, dust imprinted surface water and NADW) is the dominant factor controlling the [Al] distribution (see section 4.1.3).

As yet another argument, Measures et al. (in press) use the changing dissolved Al/Si ratio over the water column to argue the absence of Al release from biogenic particles. However, this argument cannot be based on the dissolved ratio. Biological uptake of Si and uptake and/or scavenging of Al reduces the concentrations of both elements, whereas remineralisation/release has the opposite effect. However, the dissolved ratio results from the background concentrations in the water column (i.e. in the absence of local processes), combined with the effects of uptake/scavenging and remineralisation/release. The background concentrations of Al and Si are naturally very different in the dust impacted surface ocean and the underlying masses AAIW, Mediterranean Outflow Water and NADW. Additionally, remobilisation of Al and Si at the sediment water interface releases different relative amounts of the elements compared to water column remobilisation as diagenetic processing increases the Al content, at least for biogenic opal (e.g. Gehlen et al., 2002; Koning et al., 2007). For example in the Arctic Ocean, in the deepest bottom waters close to the seafloor, the slope of the dissolved Al/Si correlation is significantly steeper (Middag et al., 2009; their Figures 5b, 8, 13a,b, 15c, 18).

4.6.2 Global Ocean

The distribution of Al in the Atlantic Ocean differs from the distributions in the Pacific Ocean (Orians and Bruland, 1986), Indian Ocean (Obata et al., 2004) and Southern Ocean (Middag et al., 2011b). The higher dust loading of the Atlantic Ocean has a profound influence on the surface and recently sub-ducted water, but there is no evidence this affects the deep concentrations (Fig. 3a, 3b and Fig 11). In the near bottom Pacific, Indian and Southern Ocean, [Al] is low (generally < 4 nmol kg^{-1}) and there is no apparent increase of Al during along-bottom advection (Middag et al., 2011b; Obata et al., 2004; Orians and Bruland, 1986). Contrarily, in the near bottom West Atlantic, the [Al] is higher (up to 23 nmol kg^{-1} deeper than 5000m) and does increase during advection along the bottom, mainly due to mixing with overlying Al-rich NADW. The lack of a similar Al-rich water mass in the other oceans combined with a net removal of Al via scavenging

(Fig. 6 and Fig. 8; see also section 4.2) probably explains the lower near bottom [Al] observed in those other basins. Future work within the GEOTRACES program will show whether there is a small increase in deep [Al] during along bottom advection after all in the other ocean basins, or whether sediment resuspension input as observed here for the AABW is sufficiently small that it is balanced by scavenging.

An interesting hypothesis to explain the different Al distributions between different deep oceans comes from the work of Mackin and Aller (1986). They suggested that [Si] in the water column is of importance and that higher [Si] in bottom waters prevents the release of Al from the underlying sediments (see also section 4.3.1). Given the high [Si] in the Southern, Indian and Pacific Oceans compared to the Atlantic this could be a factor of importance by nullifying a flux from the sediments as well as minimising the release of Al during sediment resuspension. This hypothesis was recently tested in a model study of the world oceans (van Hulten et al., 2014), which demonstrated this is a feasible explanation. Van Beusekom et al. (1997) suggested that when significant concentrations of biogenic silica are present in the surface sediments, that can act as a filter and scavenges the Al that otherwise could flux into the overlying water column. This could be important in the Southern Ocean where the lowest bottom [Al] is observed, but would be less relevant in the other oceans.

4.7. Basin-scale relationships and micro-scale mechanisms

Inspired by the GEOSECS program and the ensuing unravelling of biogeochemical processes by use of tracers in the sea (Broecker and Peng, 1982), we had chosen to study trace elements combined with the nowadays classical ocean tracers in the deep ocean conveyor belt of the West Atlantic Ocean. Here we have found intriguing relationships, or the absence thereof, of dissolved Al with dissolved Si, and also trends of Al versus salinity and AOU. In this study and in the complementary ocean circulation and biogeochemistry model simulation efforts (Van Hulten et al., 2013, 2014) several processes have become apparent. The role of deep ocean circulation is very significant, waters of Nordic origin with high Al and low Si contrasting with Antarctic source waters with low Al and high Si, together yielding a strong imprint throughout the West Atlantic Ocean. This internal circulation within the Atlantic is augmented by external sources and internal biological cycling. External sources are the long recognized Sahara dust supply and as now confirmed, a major sediment re-suspension source in the northern Northwest Atlantic Ocean. Further quantification of these external sources would benefit from high resolution sampling in surface waters and northern bottom waters, respectively, in future research. The internal cycling of Al in context of the ocean biological cycle is evident from the tracer relationship with Si and AOU. This is a step forward in understanding the cycling of Al, but does as yet not provide a firm delineation of the underlying microscopic scale mechanisms. These can be 'true' incorporation in diatom opal frustules, adsorption at outside of such frustules, and the opal ballast effect, as well as combinations thereof. With regards to the latter ballast effect please be aware that another biogenic hard shell, $CaCO_3$, also acts as ballast for settling biogenic debris, and may also play a role in the Al cycle. Future research investigating the relation between Al and carbonate alkalinity might elucidate this, but given the required normalisation to salinity and correction for nitrate this conceivably has a larger associated error then the directly measured Si. Thus far we have refrained from assessing the role of $CaCO_3$ in the cycling of Al, yet such role cannot be excluded either.

5. Conclusions

The water flowing into the Atlantic basin from the south (AAIW/uCDW and AABW) has low [Al] and naturally high [Si], showing the inverse image compared to NADW with high [Al] and low [Si] (Fig. 3a and Fig. 3b). However, upon closer inspection it becomes evident that Al and Si are not simply each other's opposites in mixing of two endmembers. In fact, Al and Si are also involved in biogeochemical relationships of an elusive nature. The ocean distribution of dissolved Al is controlled by the external sources and its internal ocean cycling. This cycling is linked with the biogenic silica cycle (or at least biogenic particles where Si-opal ballast effects play a role), but affected by the scavenging intensity, the surface concentrations of Al and Si, and the regional (external) supply of Al and/or Si. In the deep ocean the Al-Si relation changes while the water is advected along the 'ocean conveyor'. The particle-reactive nature of Al (deep water residence time 100-150 years) versus 'inert' silicate (residence time >10000 years) causes a net removal of Al from deep waters while dissolved silicate is left behind in deep waters, uncoupling the Al and Si cycling in the deep ocean. This implies a positive Al-Si relation is likely to be mostly or only observed in semi-enclosed or otherwise relatively isolated ocean regions without inflow of relatively 'old' water. Examples of such regions are the Arctic Ocean (Middag et al., 2009), the Subarctic Gyre (this work) and the Mediterranean Sea ((Chou and Wollast, 1997; Hydes et al., 1988; Rolison et al., submitted; this issue)).. Additionally, we postulated the deep scavenging intensity has to be 'just right' according to the goldilocks principle (Bruland et al., 2014). More research is needed to establish the appropriate scavenging intensity quantitatively. The slope of the correlation between [Al] and [Si] in the Subarctic Gyre suggests release of both Al and Si from remineralising diatom frustules, but reversible scavenging on biogenic opal or other biogenic particles can explain the observed distribution as well.

Overall, this Atlantic study together with our recent polar studies (Middag et al., 2009; Middag et al., 2011b; Middag et al., 2012; Middag et al., 2013) clearly demonstrates that modern ultraclean sampling and filtration and analyses of filtered seawater yielding high accuracy data of dissolved Al are pivotal for understanding the ocean cycling of dissolved Al. The 'traditional' understandings of the cycling of Al (also based on sometimes unfiltered samples and with occasional reported or suspected contamination problems as well), inevitably are being replaced by new paradigms (Kuhn, 1962).

The dissolved Al definitely is a scavenged type element (Bruland et al., 2014), but can also display a nutrient-type profile and its cycling can be linked to the cycling of Si. However, this link is often masked by other ocean processes. The behaviour of Al in the deep ocean is not conservative on the time scale of water mass advection and it therefore is deemed unlikely Al can reliably be used as a quantitative water mass tracer. The high dust loading of the Atlantic Ocean does have a profound influence on the surface and recently sub-ducted water, but there is no evidence this affects the NADW concentrations of Al. The enrichment of Al in NADW has a distinctive sediment resuspension rather than atmospheric origin. Sediment resuspension input of Al to the deep ocean is more important than previously realised, but more work needs to be done to exactly constrain the spatial heterogeneity in apparent sediment resuspension Al input to the global deep ocean. Possible explanations include higher dissolved Si of near bottom waters preventing Al mobilization from sediments, and/or the particulate biogenic silica concentrations in the top sediment suppressing release of Al from the sediments.

References

Armstrong, R.A., Lee, C., Hedges, J.I., Honjo, S. and Wakeham, S.G., 2001. A new, mechanistic model for organic carbon fluxes in the ocean based on the quantitative association of POC with ballast minerals. Deep Sea Research Part II: Topical Studies in Oceanography, 49(1–3): 219-236.

Bainbridge, A.E., Broecker, W.S., Spencer, D. and Harmon, H., 1981. Hydrographic Data, 1972-1973. Geosecs Atlantic Ocean Expedition. National Science Foundation, Washington D.C.

Baker, A.R. and Croot, P.L., 2010. Atmospheric and marine controls on aerosol iron solubility in seawater. Marine Chemistry, 120(1-4): 4-13.

Baker, A.R., Jickells, T.D., Witt, M. and Linge, K.L., 2006. Trends in the solubility of iron, aluminium, manganese and phosphorus in aerosol collected over the Atlantic Ocean. Marine Chemistry, 98(1): 43-58.

Biscaye, P.E. and Eittreim, S.L., 1977. Suspended particulate loads and transports in the nepheloid layer of the abyssal Atlantic Ocean. Marine Geology, 23(1-2): 155-172.

Broecker, W.S., 1991. The great ocean conveyor. Oceanography, 4(2): 79–89.

Broecker, W.S. and Peng, T.H., 1982. Tracers in the Sea. Lamont-Doherty Geological Observatory, New York, 690 pp.

Brown, M.T. and Bruland, K.W., 2008. An improved flow-injection analysis method for the determination of dissolved aluminum in seawater. Limnology and Oceanography-Methods, 6: 87-95.

Bruland, K.W., Middag, R. and Lohan, M.C., 2014. 8.2 - Controls of Trace Metals in Seawater. In: H.D. Holland and K.K. Turekian (Editors), Treatise on Geochemistry (Second Edition). Elsevier, Oxford, pp. 19-51.

Brzezinski, M.A., 1985. The Si:C:N ratio of diatoms: interspecific variability and the effect of some environmental variables. Journal of Phycology, 21(3): 347-357.

Chou, L. and Wollast, R., 1997. Biogeochemical behavior and mass balance of dissolved aluminum in the western Mediterranean Sea. Deep-Sea Research Part Ii-Topical Studies in Oceanography, 44(3-4): 741-768.

Collier, R. and Edmond, J., 1984. The Trace-Element Geochemistry of Marine Biogenic Particulate Matter. Progress in Oceanography, 13(2): 113-199.

Cutter, G.A. and Bruland, K.W., 2012. Rapid and noncontaminating sampling system for trace elements in global ocean surveys. Limnology and Oceanography-Methods, 10: 425-436.

Dammshaeuser, A., Wagener, T. and Croot, P.L., 2011. Surface water dissolved aluminum and titanium: Tracers for specific time scales of dust deposition to the Atlantic? Geophysical Research Letters, 38.

De Baar, H.J.W. et al., 2008. Titan: A new facility for ultraclean sampling of trace elements and isotopes in the deep oceans in the international Geotraces program. Marine Chemistry, 111(1-2): 4-21.

Deng, F., Thomas, A.L., Rijkenberg, M.J.A. and Henderson, G.M., 2014. Controls on seawater Pa-231, Th-230 and Th-232 concentrations along the flow paths of deep waters in the Southwest Atlantic. Earth and Planetary Science Letters, 390: 93-102.

Dickson, R.R. and Brown, J., 1994. The production of North-Atlantic Deep-Water - sources, rates and patways. Journal of Geophysical Research-Oceans, 99(C6): 12319-12341.

Donners, J., Drijfhout, S.S. and Hazeleger, W., 2005. Water mass transformation and subduction in the South Atlantic. Journal of Physical Oceanography, 35(10): 1841-1860.

Dulaquais, G. et al., 2014. Contrasting biogeochemical cycles of cobalt in the surface western Atlantic Ocean. Global Biogeochemical Cycles: 2014GB004903.

Elderfield, H. and Schultz, A., 1996. Mid-ocean ridge hydrothermal fluxes and the chemical composition of the ocean. Annual Review of Earth and Planetary Sciences, 24: 191-224.

Gao, Y., Kaufman, Y.J., Tanre, D., Kolber, D. and Falkowski, P.G., 2001. Seasonal distributions of aeolian iron fluxes to the global ocean. Geophysical Research Letters, 28(1): 29-32.

Gehlen, M. et al., 2002. Unraveling the atomic structure of biogenic silica: Evidence of the structural association of Al and Si in diatom frustules. Geochimica Et Cosmochimica Acta, 66(9): 1601-1609.

Grasshoff, K., Erhardt, M. and Kremling, K., 1983. Methods in Seawater Analyses. Verlag Chemie, Weinheim, Germany.

Hall, I.R. and Measures, C.I., 1998. The distribution of Al in the IOC stations of the North Atlantic and Norwegian Sea between 52 degrees and 65 degrees North. Marine Chemistry, 61(1-2): 69-85.

Han, Q., Moore, J.K., Zender, C., Measures, C. and Hydes, D., 2008. Constraining oceanic dust deposition using surface ocean dissolved Al. Global Biogeochemical Cycles, 22(2): 14.

Honjo, S., Manganini, S.J., Krishfield, R.A. and Francois, R., 2008. Particulate organic carbon fluxes to the ocean interior and factors controlling the biological pump: A synthesis of global sediment trap programs since 1983. Progress in Oceanography, 76(3): 217-285.

Hydes, D.J., 1979. Aluminum in seawater - control by inorganic processes. Science, 205(4412): 1260-1262.

Hydes, D.J., Delange, G.J. and Debaar, H.J.W., 1988. Dissolved aluminium in the Mediterranean. Geochimica Et Cosmochimica Acta, 52(8): 2107-2114.

Klunder, M.B., Laan, P., Middag, R., de Baar, H.J.W. and Bakker, K., 2012. Dissolved iron in the Arctic Ocean: Important role of hydrothermal sources, shelf input and scavenging removal. Journal of Geophysical Research-Oceans, 117.

Klunder, M.B., Laan, P., Middag, R., De Baar, H.J.W. and van Ooijen, J.C., 2011. Dissolved iron in the Southern Ocean (Atlantic sector). Deep-Sea Research Part Ii-Topical Studies in Oceanography, 58(25-26): 2678-2694.

Koning, E., Gehlen, M., Flank, A.M., Calas, G. and Epping, E., 2007. Rapid post-mortem incorporation of aluminum in diatom frustules: Evidence from chemical and structural analyses. Marine Chemistry, 106(1-2): 208-222.

Kramer, J., Laan, P., Sarthou, G., Timmermans, K.R. and de Baar, H.J.W., 2004. Distribution of dissolved aluminium in the high atmospheric input region of the subtropical waters of the North Atlantic Ocean. Marine Chemistry, 88(3-4): 85-101.

Kuhn, T.S., 1962. The structure of scientific revolutions. The University of Chicago Press, Chicago, 210 pp.

Lam, P.J., Ohnemus, D.C. and Auro, M.E., in press. Size-fractionated major particle composition and concentrations from the US GEOTRACES north Atlantic zonal transect. Deep Sea Research Part II: Topical Studies in Oceanography(0).

Li, F. et al., 2013. The biogeochemical behavior of dissolved aluminum in the southern Yellow Sea: Influence of the spring phytoplankton bloom. Chinese Science Bulletin, 58(2): 238-248.

Lunel, T., Rudnicki, M., Elderfield, H. and Hydes, D., 1990. Aluminum as a depth-sensitive tracer of entrainment in submarine hydrothermal plumes. Nature, 344(6262): 137-139.

Mackin, J.E. and Aller, R.C., 1986. The effects of clay mineral reactions on dissolved Al distributions in sediments and waters of the Amazon Continental-Shelf. Continental Shelf Research, 6(1-2): 245-262.

Mahowald, N.M. et al., 2002. Understanding the 30-year Barbados desert dust record. Journal of Geophysical Research-Atmospheres, 107(D21).

Maring, H.B. and Duce, R.A., 1987. The impact of atmospheric aerosols on trace-metal chemistry in open ocean surface seawater. 1. Aluminum Earth and Planetary Science Letters, 84(4): 381-392.

Measures, C., Hatta, M., Fitzsimmons, J. and Morton, P., in press. Dissolved Al in the zonal N Atlantic section of the US GEOTRACES 2010/2011 cruises and the importance of hydrothermal inputs. Deep Sea Research Part II: Topical Studies in Oceanography(0).

Measures, C.I., 1995. The distribution of Al in the IOC stations of the eastern Atlantic between 30 ° S and 34 ° N. Marine Chemistry, 49(4): 267-281.

Measures, C.I., 2013. Shipboard FIA dissolved Al, Fe, and Mn (0.2 um AcroPak filter) from cruise KN204-01 (GT11) & Shipboard FIA dissolved Al and Fe (0.2 um AcroPak filter) from cruise KN199-04 (GT10). Biological and Chemical Oceanography Data System. BCO-DMO, WHOI. . iPub: 14 October 2013. Accessed: 15 January 2015, http://data.bco-dmo.org/jg/dir/BCO/GEOTRACES/NorthAtlanticTransect/.

Measures, C.I. and Brown, E.T., 1996. Estimating dust input to the Atlantic Ocean using surface water aluminium concentrations. Impact of Desert Dust across the Mediterranean, 11, 301-311 pp.

Measures, C.I., Landing, W.M., Brown, M.T. and Buck, C.S., 2008. High-resolution Al and Fe data from the Atlantic Ocean CLIVAR-CO2 repeat hydrography A16N transect: Extensive linkages between atmospheric dust and upper ocean geochemistry. Global Biogeochemical Cycles, 22(1).

Measures, C.I. and Vink, S., 2000. On the use of dissolved aluminum in surface waters to estimate dust deposition to the ocean. Global Biogeochemical Cycles, 14(1): 317-327.

Middag, R., 2010. Dissolved Aluminium and Manganese in the Polar Oceans, University of Groningen, Groningen, the Netherlands, 237 pp.

Middag, R. et al., submitted. Intercomparison of Dissolved Trace Elements at the Bermuda Atlantic Time Series Station.

Middag, R., de Baar, H.J.W., Klunder, M.B. and Laan, P., 2013. Fluxes of dissolved aluminum and manganese to the Weddell Sea and indications for manganese co-limitation. Limnology and Oceanography, 58(1): 287-300.

Middag, R., de Baar, H.J.W., Laan, P. and Bakker, K., 2009. Dissolved aluminium and the silicon cycle in the Arctic Ocean. Marine Chemistry, 115(3-4): 176-195.

Middag, R., de Baar, H.J.W., Laan, P., Cai, P.H. and van Ooijen, J.C., 2011a. Dissolved manganese in the Atlantic sector of the Southern Ocean. Deep-Sea Research Part Ii-Topical Studies in Oceanography, 58(25-26): 2661-2677.

Middag, R., de Baar, H.J.W., Laan, P. and Huhn, O., 2012. The effects of continental margins and water mass circulation on the distribution of dissolved aluminum and manganese in Drake Passage. Journal of Geophysical Research-Oceans, 117.

Middag, R., van Slooten, C., de Baar, H.J.W. and Laan, P., 2011b. Dissolved aluminium in the Southern Ocean. Deep-Sea Research Part Ii-Topical Studies in Oceanography, 58(25-26): 2647-2660.

Moran, S.B. and Moore, R.M., 1988. Temporal variations in dissolved and particulate aluminium during a spring bloom. Estuarine Coastal and Shelf Science, 27(2): 205-215.

Moran, S.B. and Moore, R.M., 1991. The potential source of dissolved aluminum from resuspended sediments to the North-Atlantic Deep-Water. Geochimica Et Cosmochimica Acta, 55(10): 2745-2751.

Moran, S.B. and Moore, R.M., 1992. Kinetics of the removal of dissolved aluminum by diatoms in seawater - a comparison with thorium Geochimica Et Cosmochimica Acta, 56(9): 3365-3374.

Nelson, D.M. et al., 2002. Vertical budgets for organic carbon and biogenic silica in the Pacific sector of the Southern Ocean, 1996-1998. Deep-Sea Research Part Ii-Topical Studies in Oceanography, 49(9-10): 1645-1674.

Nelson, D.M., Tréguer, P., Brzezinski, M.A., Leynaert, A. and Quéguiner, B., 1995. Production and dissolution of biogenic silica in the ocean: Revised global estimates, comparison with regional data and relationship to biogenic sedimentation. Global Biogeochemical Cycles, 9(3): 359-372.

Obata, H., Nozaki, Y., Alibo, D.S. and Yamamoto, Y., 2004. Dissolved Al, In, and Ce in the eastern Indian Ocean and the Southeast Asian Seas in comparison with the radionuclides Pb-210 and Po-210. Geochimica Et Cosmochimica Acta, 68(5): 1035-1048.

Orians, K.J. and Bruland, K.W., 1985. Dissolved Aluminum in the Central North Pacific. Nature, 316(6027): 427-429.

Orians, K.J. and Bruland, K.W., 1986. The biogeochemistry of aluminium in the Pacific-Ocean. Earth and Planetary Science Letters, 78(4): 397-410.

Orians, K.J. and Bruland, K.W., 1988. The Marine Geochemistry of Dissolved Gallium - a Comparison with Dissolved Aluminum. Geochimica Et Cosmochimica Acta, 52(12): 2955-2962.

Provost, C., Escoffier, C., Maamaatuaiahutapu, K., Kartavtseff, A. and Garcon, V., 1999. Subtropical mode waters in the South Atlantic Ocean. Journal of Geophysical Research-Oceans, 104(C9): 21033-21049.

Redfield, A.C., Ketchum, B.H. and Richards, F.A., 1963. The influence of organisms on the composition of seawater. In: H.M. N. (Editor), The Sea, Volume 2: The Composition of Sea-Water Comparative and Descriptive Oceanography. Harvard University Press, New York, USA, pp. 26-77.

Rijkenberg, M.J.A. et al., 2014. The Distribution of Dissolved Iron in the West Atlantic Ocean. Plos One, 9(6).

Roberts, K., Granum, E., Leegood, R.C. and Raven, J.A., 2007. Carbon acquisition by diatoms. Photosynthesis Research, 93(1-3): 79-88.

Rolison, J.M., Middag, R., Stirling, C., Rijkenberg, M.J.A. and De Baar, H.J.W., submitted; this issue. Zonal distribution of dissolved aluminium in the Mediterranean Sea.

Rudels, B., Muench, R.D., Gunn, J., Schauer, U. and Friedrich, H.J., 2000. Evolution of the Arctic Ocean boundary current north of the Siberian shelves. Journal of Marine Systems, 25(1): 77-99.

Sarmiento, J.L. and Gruber, N., 2006. Ocean Biogeochemical Dynamics Princeton University Press, Princeton, New Jersey.

Stoffyn, M., 1979. Biological-control of dissolved aluminum in seawater - experimental-evidence. Science, 203(4381): 651-653.

Stramma, L., 1989. THE BRAZIL CURRENT TRANSPORT SOUTH OF 23-DEGREES-S. Deep-Sea Research Part a-Oceanographic Research Papers, 36(4): 639-646.

Stramma, L. and England, M.H., 1999. On the water masses and mean circulation of the South Atlantic Ocean. Journal of Geophysical Research-Oceans, 104(C9): 20863-20883.

Sunda, W.G. and Huntsman, S.A., 1988. Effect of sunlight on the redox cycles of manganese in the southwestern Sargasso Sea. Deep-Sea Research Part a-Oceanographic Research Papers, 35(8): 1297-1317.

The GEOTRACES group, submitted. The GEOTRACES Intermediate Data Product 2014. Marine Chemistry.

Treguer, P.J. and De La Rocha, C.L., 2013. The World Ocean Silica Cycle. Annual Review of Marine Science, Vol 5, 5: 477-501.

Van Aken, H.M., 2007. The Oceanic Thermohaline Circulation: An Introduction. Springer Science + Business Media, New York, USA.

Van Aken, H.M. and De Boer, C.J., 1995. On the synoptic hydrography of intermediate and deep-water masses in the iceland basin. Deep-Sea Research Part I-Oceanographic Research Papers, 42(2): 165-189.

Van Beusekom, J.E.E., Van Bennekom, A.J., Treguer, P. and Morvan, J., 1997. Aluminium and silicic acid in water and sediments of the Enderby and Crozet Basins. Deep-Sea Research Part Ii-Topical Studies in Oceanography, 44(5): 987-1003.

van Hulten, M.M.P. et al., 2014. On the effects of circulation, sediment resuspension and biological incorporation by diatoms in an ocean model of aluminium. Biogeosciences, 11(14): 3757-3779.

Van Hulten, M.M.P. et al., 2013. Aluminium in an ocean general circulation model compared with the West Atlantic Geotraces cruises. Journal of Marine Systems, 126: 3-23.

Vrieling, E.G., Poort, L., Beelen, T.P.M. and Gieskes, W.W.C., 1999. Growth and silica content of the diatoms Thalassiosira weissflogii and Navicula salinarum at different salinities and enrichments with aluminium. European Journal of Phycology, 34(3): 307-316.

Worthington, L.V., 1959. The 18-degree water in the Sargasso Sea. Deep-Sea Research, 5(4): 297-305.

Worthington, L.V., 1976. On the North Atlantic Circulation Johns Hopkins University Press, Baltimore, Maryland.

Worthington, L.V., 1981. The water masses of the world ocean: some results of a fine-scale census. In: W. B.A. and W. C. (Editors), Evolution of Physical Oceanography. MIT Press, Cambridge, Massachusetts.

Table 1 Results for the SAFe and GEOTRACES reference samples with standard deviation (±) and number of triplicate analyses (n). Consensus values are the May 2013 values (http://www.geotraces.org/science/intercalibration/322-standards-and-reference-materials) with standard deviation (±) and number of participation laboratories (n).

Al (nmol/kg)	Safe S	GEOTRACES GS	GEOTRACES GD
This study	1.68±0.03 (n=4)	27.4±0.3 (n=12)	17.5±0.3 (n=21)
Consensus values	1.67±0.1 (n=6)	27.5±0.2 (n=6)	17.7±0.2 (n=6)

Table 2 Thermohaline water mass properties along the western Atlantic GEOTRACES section

Water Mass	Dominant region	S range	Θ range (^{0} C)
DSW	50° - 64°N	34.88 – 34.90	1.22 – 2.02
ISOW	54° - 63°N	34.926 – 34.932	2.63 – 2.88
LSW	51° - 63°N	34.86 – 34.89	3.54 – 3.73
NACW	15° - 43°N	35.30 – 37.12	10.0 – 23.0
STMW Northern Hemisphere	20° - 35°N	36.4 – 36.6	17.0 – 19.0
STMW Southern Hemisphere	36° - 28°S	35.0 – 35.6	11.5 – 15.0
NADW	36°S - 40°N	34.89 – 34.99	2.0 - 4.2
AAIW	48°S - 15°N	34.15 – 34.76	3.57 – 6.31
uCDW	48°S - 15°N	34.52 – 34.81	2.56 – 5.30
AABW	49°S - 30°N	34.77 – 34.87	-0.16 – 1.70

These properties are based on hydrographical observations along the transect and the Atlantic Ocean in general (Van Aken, 2007). These properties are for the cores of the water masses in the regions where the water mass is a dominant feature and are valid for the years the observations were made.

Table 3 Al-Si, Al-salinity (Al-Sal), Al-Θ, Si-salinity Si-Sal) and Si-Θ relationships for the upper, middle and lower neutral density ranges (±0.005 kg m^{-3} average value given) of the NADW in the northern most latitude zone (see Fig. 4). Neutral density ranges were chosen to maximise the number of data points in the upper, middle and lower neutral density ranges.

	Upper (27.830 kg m^{-3}) n=6	Middle (27.925 kg m^{-3}) n=8	Deep (28.035 kg m^{-3}) n=6
Al-Si	[Al]=2.3[Si] – 15.4 R^2=0.83	[Al]=3.2[Si] – 25.4 R^2=0.93	[Al]=1.7[Si] - 6.5 R^2=0.86
Al-Sal	[Al]=490xSal - 1705 R^2=0.72	[Al]=110xSal - 3828 R^2=0.90	[Al]=-270xSal + 9454 R^2=0.34
Al-Θ	[Al]=7.5x Θ - 27 R^2=0.65	[Al]=13.6x Θ - 38 R^2=0.56	[Al]=-4.2x Θ + 131 R^2=0.76
Si-Sal	[Si]=16xSal - 557 R^2=0.50	[Si]=32.3xSal - 1117 R^2=0.88	[Si]=-124xSal + 4330 R^2=0.24
Si-Θ	[Si]=2.4x Θ – 1.2 R^2=0.42	[Si]=3.9x Θ – 2.9 R^2=0.54	[Si]=-19.8x Θ + 68 R^2=0.55

Figure captions

Figure 1 Previously postulated hypothesis for changes in the NADW when flowing southwards. Adsorptive scavenging causes continuous removal of Al from deep waters, while 'inert' dissolved Si only continues to increase due to dissolution of sinking diatom frustules. As a result the slope $\Delta Al/\Delta Si$ decreases steadily while NADW travels from the Northern Hemisphere (NH) to the Southern Hemisphere (SH).

Figure 2 Sampling stations. With a total of 60 full water column depth profiles sampled, the transect was completed in four separate cruises. Stations 1.2 -1.19 were sampled during cruise 64 PE 319 aboard RV Pelagia in April/May 2010 (blue dots). Stations 2.21-2.41 were sampled during cruise 64PE321 (black dots) in June/July 2010 and stations 4.3-4.7 were sampled during cruise 64PE358 (yellow dots) in August 2012 aboard RV Pelagia completing sampling in the Northern Hemisphere. Latter cruise in 2012 was to sample at 5 stations that had to be skipped in the first cruise (April/May2010) due to heavy storms at those stations (sampling is feasible at sea states corresponding to wind velocity < 17 m/s i.e. < Bft 8). Sampling of the GA02 GEOTRACES transect in the Southern Hemisphere was conducted from the Bristish research vessel RRS James Cook (cruise 74JC057) in March/April 2011 (red dots). Numbers in this figure indicate the leg and station numbers (leg#.Station#).

Figure 3. Distributions of dissolved aluminium, nitrate and silicate and dissolved oxygen overlain with salinity and neutral density. 3a Distribution of dissolved Al (nmol/kg) in colour scale overlain with isohalines for salinity. 3b Distribution of silicate (Si in µmol/kg) in colour scale overlain with salinity isobars. 3c Distribution of nitrate (NO_3 in µmol/kg) in colour scale overlain with isohalines for salinity. 3d Distribution of dissolved Al (nmol/kg) in colour scale overlain with isohalines for neutral density (γ^n, kg m^{-3}). 3e Distribution of silicate (Si in µmol/kg) in colour scale overlain with neutral density isobars (γ^n, kg m^{-3}). 3f Distribution of dissolved oxygen (O_2 in µmol/kg) overlain with neutral density isobars (γ^n, kg m^{-3}). Dots represent sampled depths for Al, Si and NO_3. Salinity, neutral density and oxygen are sensor data from the CTD downcasts. Refer to Table 2 for thermohaline water mass properties along the western Atlantic GEOTRACES section. Acronyms: AABW: Antarctic Bottom Water; AAIW: Antarctic Intermediate Water; DSOW: Denmark Strait Overflow Water; ISOW: Iceland-Scotland Overflow Water; LSW: Labrador Sea Water; NACW: North Atlantic Central Water; NADW: North Atlantic Deep Water; uCDW: upper Circumpolar Deep Water; STMW: Subtropical Mode Water.

Figure 4 The boundaries of the major water masses NADW, LSW/ISOW and DSOW as used in this paper. Shown in colors black, grey, red, blue and green is the subdivision of NADW (and its precursors) in five latitude zones for the five linear regressions in Figures 5 and 6. For the black zone (fat black dots, DSOW excluded), all data points below 150 m depth and shallower than DSOW were used, i.e. between the surface layer and the DSOW (salinity<34.90), including the relatively fresh LSW at intermediate depths (Table2). From about 51°49'N (station 1.9) the saline STMW is found in the subsurface and all deep water column data with a salinity <34.9 (to exclude relatively fresh DSOW that is affected by sediment input) and upper water column data points with salinity >34.95 (to exclude the salty STMW with high Al related to atmospheric input) were excluded (relatively fresh LSW at intermediate depths is included). In the grey and red zone, all data with a salinity >34.89 (to exclude relatively fresh AABW with high Si and low Al) and a salinity <35 (to exclude the salty surface water) was considered NADW. From about 16°50'N (station 2.31) the upper cut-off of a salinity <35 is not correct anymore due to the

presence of relatively fresh AAIW/UCDW and the salinity maximum was used as a cut-off instead (the transition from NADW to the overlying low salinity water is recognizable as a salinity maximum). The same cut-offs are used for the blue and green zone.

Figure 5 Aluminum and silicate in the Subarctic Gyre. 5a Concentrations of Al (nmol/kg) versus Si (µmol/kg) in the Subarctic Gyre in the subsurface and intermediate water column with depth in colour scale. See figure 4 for data points used (fat black dots). 5b Concentrations of Al (nmol/kg) and Si (µmol/kg) versus salinity using the same data points as in Figure 5a. 5c Concentrations of Al (nmol/kg) versus Si (µmol/kg) in the Subarctic Gyre at a γ^n interval of 0.01 kg m^{-3} at 27.925 kg m^{-3}. This isopycnal encompassed data from the northern to the southern edge of the Subarctic Gyre. Water at this isopycnal sunk from ~1500m in the north to ~ 2000 m on the southern edge of the Gyre; the smaller number of data points (8) compared to number of sampled stations in the Subarctic Gyre is the result of the sampling resolution, i.e. this isopycnal was not sampled at 6 stations. The relationship is described by [Al]= 3.2 [Si]-25.4, with R^2=0.93; p < 0.001 and n=8. Neutral density (γ^n, kg m^{-3}) is represented in the colour scale.

Figure 6 Aluminium and silicate in North Atlantic Deep Water. For samples in the core of the southward flowing NADW (see Figure 4 for data points in corresponding colour scale), the slope of correlation of [Al] (nmol/kg) versus [Si] (µmol/kg) decreases from north to south from 0.63 10^{-3} to 0.21 10^{-3} and the goodness of fit also deteriorates going southwards from R^2> 0.90 to R^2=0.64 but linearity remains significant. The change in slope of the relation in this figure indicates net scavenging loss of Al and a net increase of Si due to remineralisation. All regressions, n=93; n=66; n=22; and n=39 for the grey, red, blue and green regression, respectively, are significant with a P < 0.001.

Figure 7 Aluminium in the oxygen minimum zone. 7a Vertical profiles of Al (nmol/kg) and oxygen (µmol/kg) concentration in the oxygen minimum zone for the three stations just north of the equator (left to right 4°N, 2.5°N and 1°N (stations 2.38, 2.39 and 2.40)). 7b Apparent oxygen utilisation (AOU) (µmol/kg) versus [Al] (nmol/kg) in the centre of the oxygen minimum zone (AOU>150 µmol kg^{-1}) between 200 and 800 m depth (Fig. 7a) between 10°N and the equator.

Figure 8 The deep and intermediate water south of 40°N with latitude in color scale (negative latitudes denote the Southern Hemisphere). Data points were selected from the deepest sampled depth till the Si minimum around 1750-2000 m depth (deepening to ~3000 m depth south of 26°S) to exclude the AAIW/uCDW influence with a salinity range that overlaps with the deeper water masses (AABW/lNADW). The uCDW/AAIW shows as an Si max, the underlying Si minimum is related to uNADW. 8a Potential temperature θ (°C) versus salinity. 8b [Si] (µmol kg^{-1}) versus salinity. 8c [Al] (nmol kg^{-1}) versus salinity. 8d [Al] (nmol kg^{-1}) versus neutral density (γ^n, kg m^{-3}).

Figure 9 Bottom water Al and Si in the subarctic gyre. Upper panel: Bottom (deepest sample) concentrations of Al (nmol kg^{-1}) and Si (µmol kg^{-1}) versus latitude in the subarctic gyre region show an increase of dissolved Al in southwards flowing DSOW until at ~45 °S. This becomes underlain by AABW influenced bottom water with a much higher dissolved Si that prevents any further dissolution of Al into the AABW. Bottom panel: Correlation between bottom Al (nmol kg^{-1}) and latitude (P<0.001 and R^2=0.95 for n=13 data points) in the DSOW in the 45-65 °N region where DSOW is the bottom water.

Figure 10 Beam attenuation coefficient in the deep and intermediate water column along the transect. Higher attenuation is indicative of more suspended particles in the water column.

Figure 11 Distribution of dissolved Al (nmol/kg) in color scale overlain with neutral density isopycnals. STMW: Subtropical Mode Water.

Fig. 1

Fig. 2

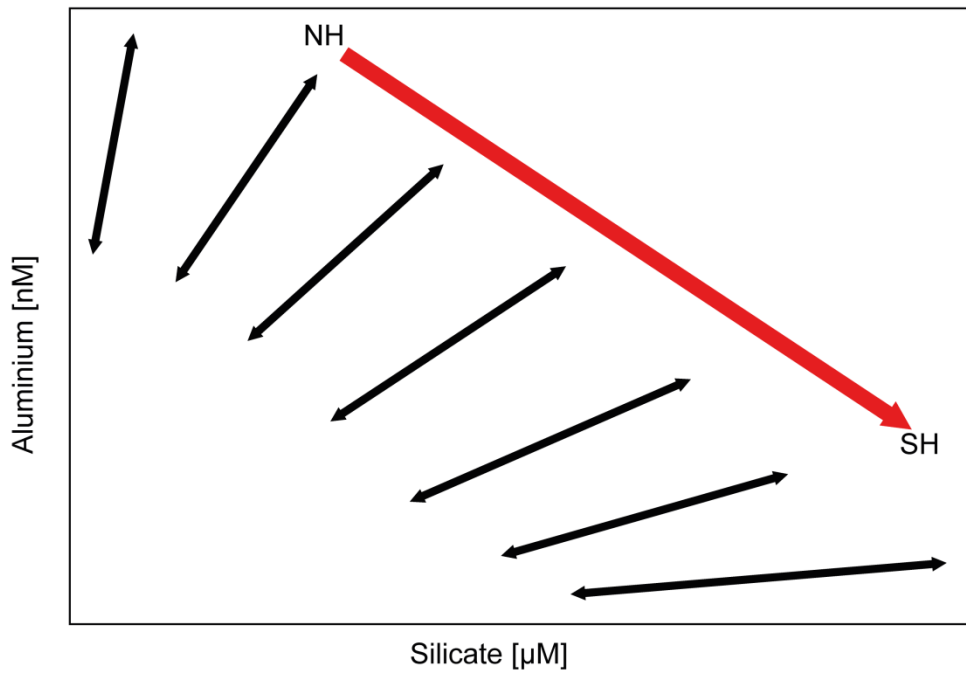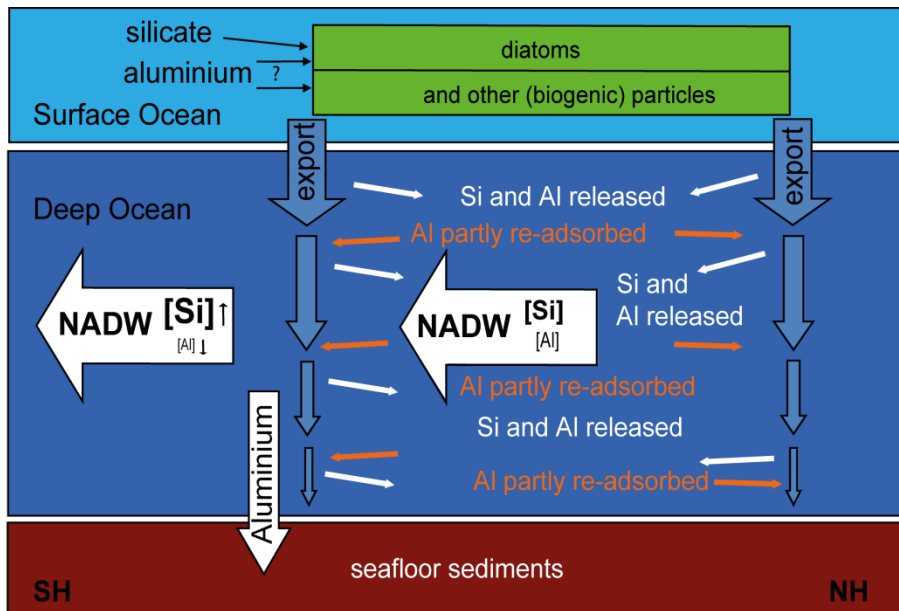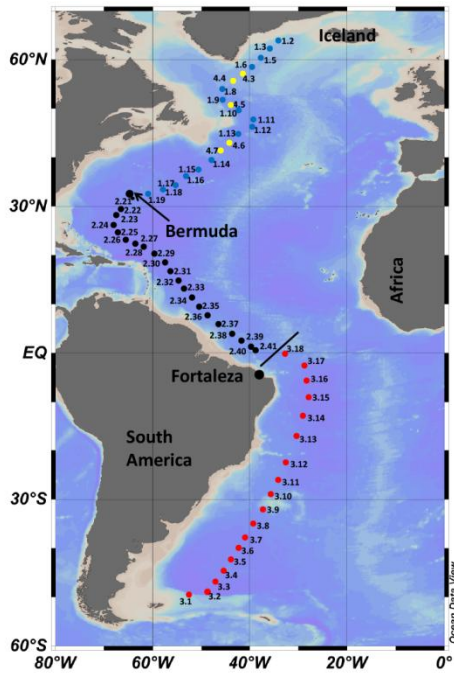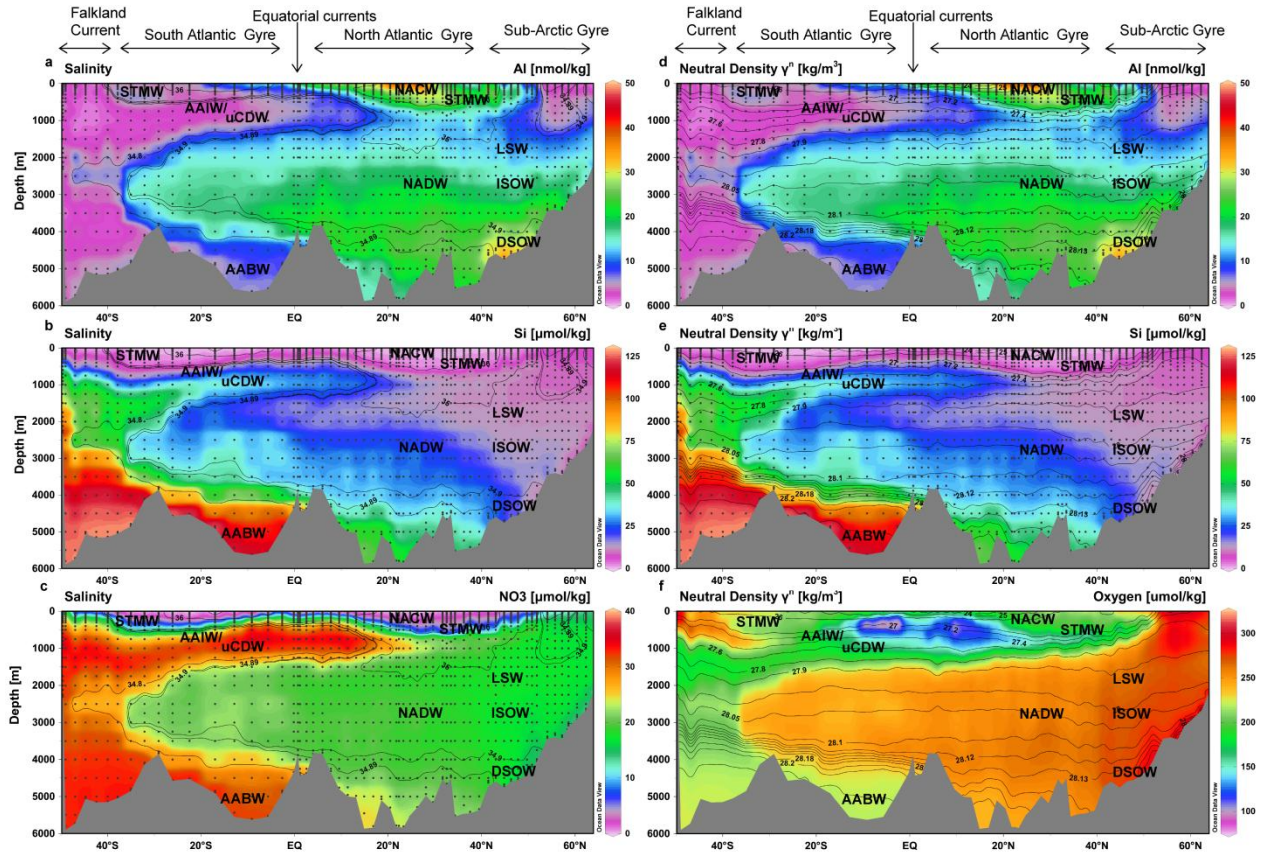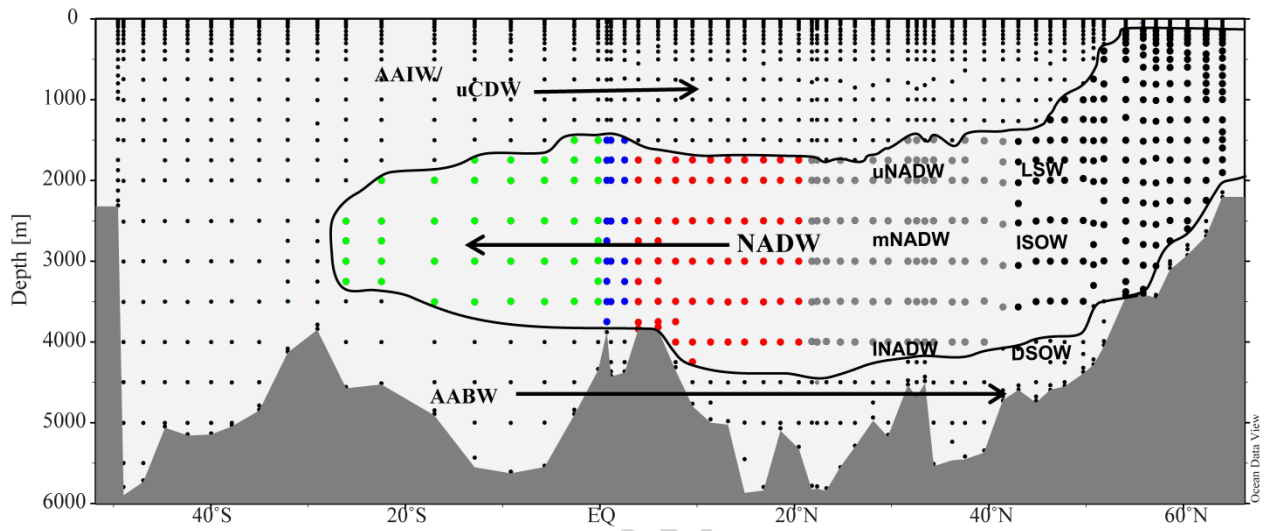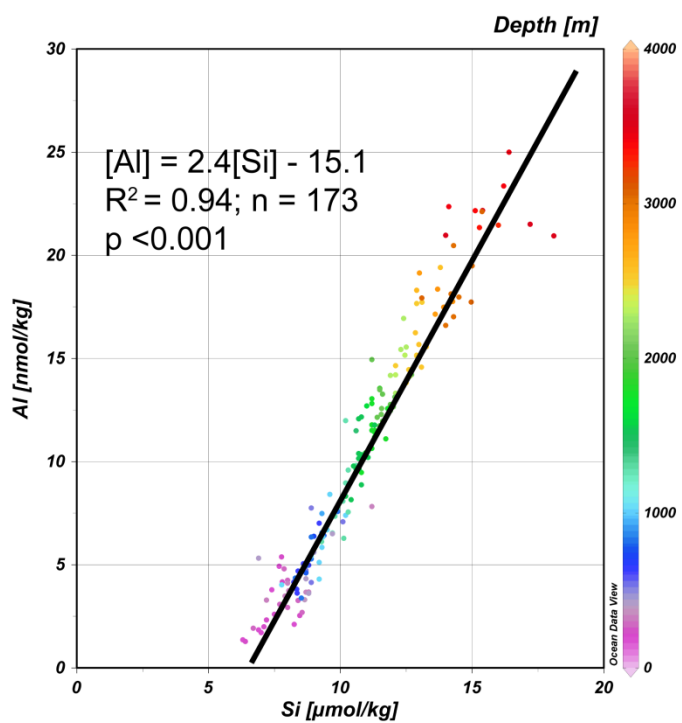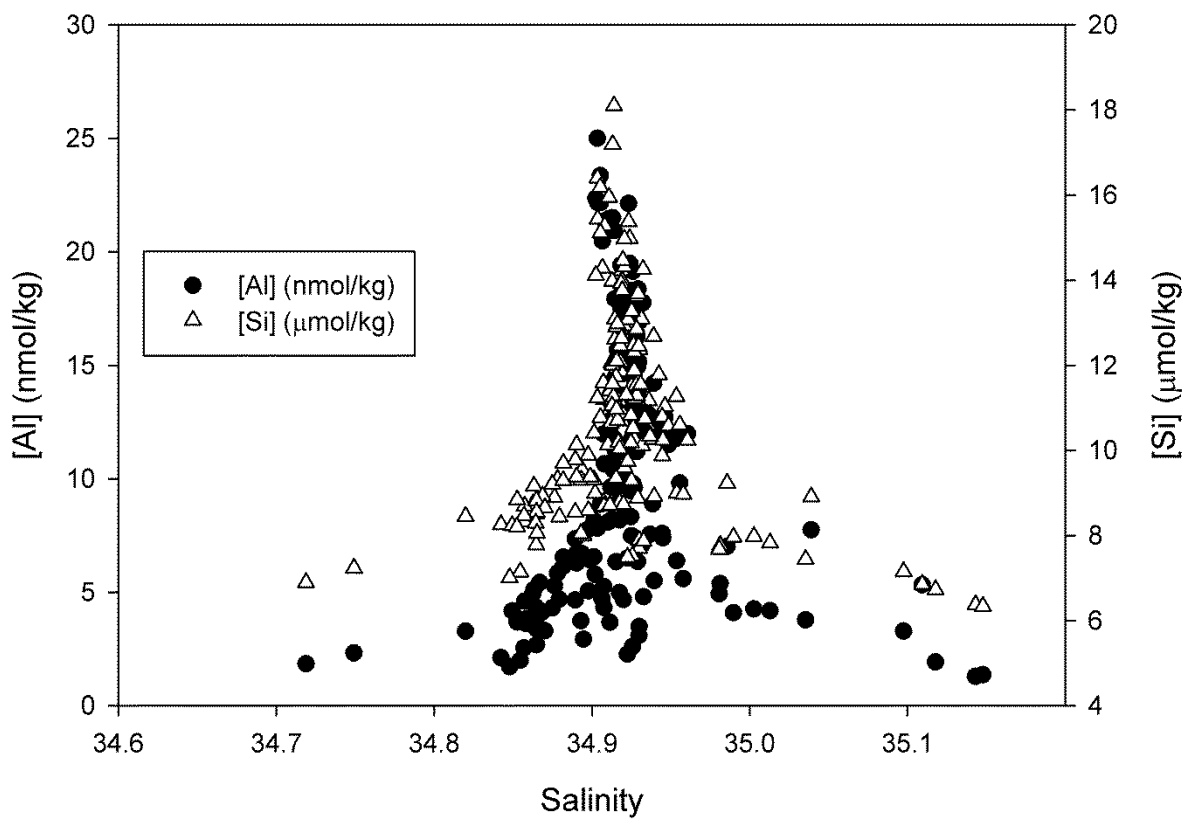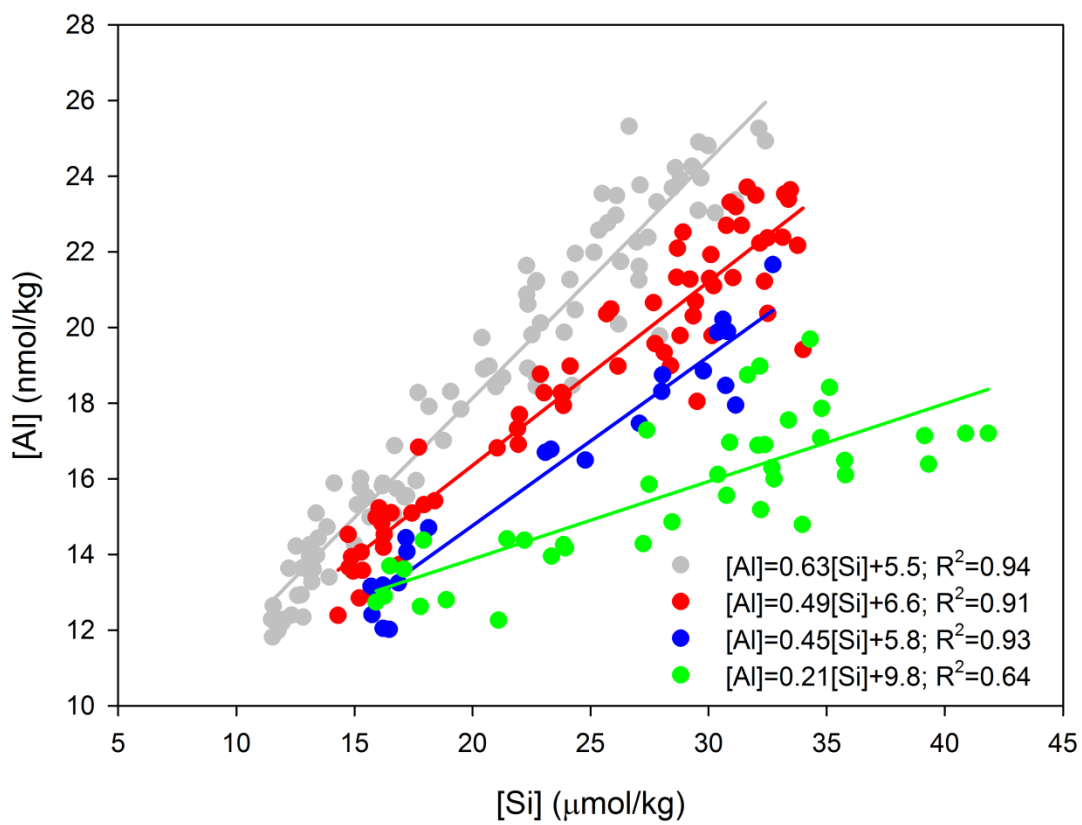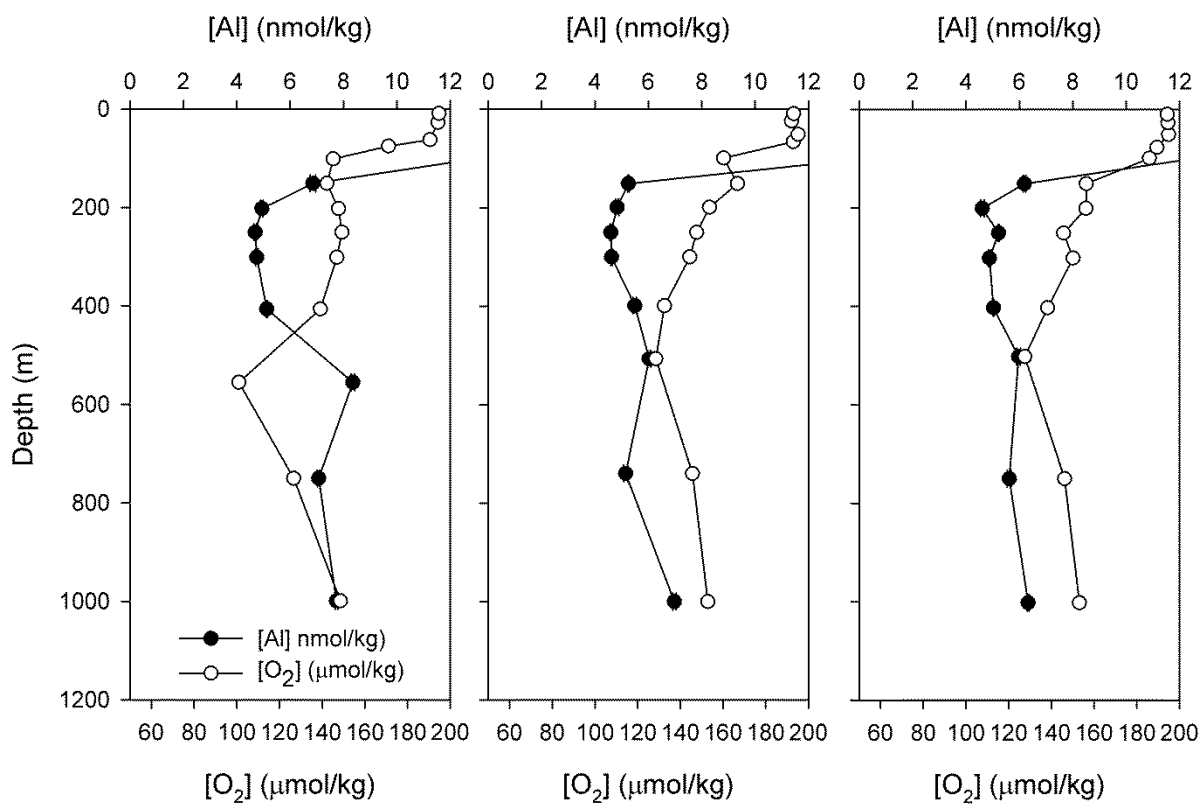Fig. 3

Fig. 4

Fig. 5a

Fig. 5b

Fig. 5c

Fig. 6

The figure legend shows the following regression equations:

[Al]=0.63[Si]+5.5; R^2=0.94

[Al]=0.49[Si]+6.6; R^2=0.91

[Al]=0.45[Si]+5.8; R^2=0.93

[Al]=0.21[Si]+9.8; R^2=0.64

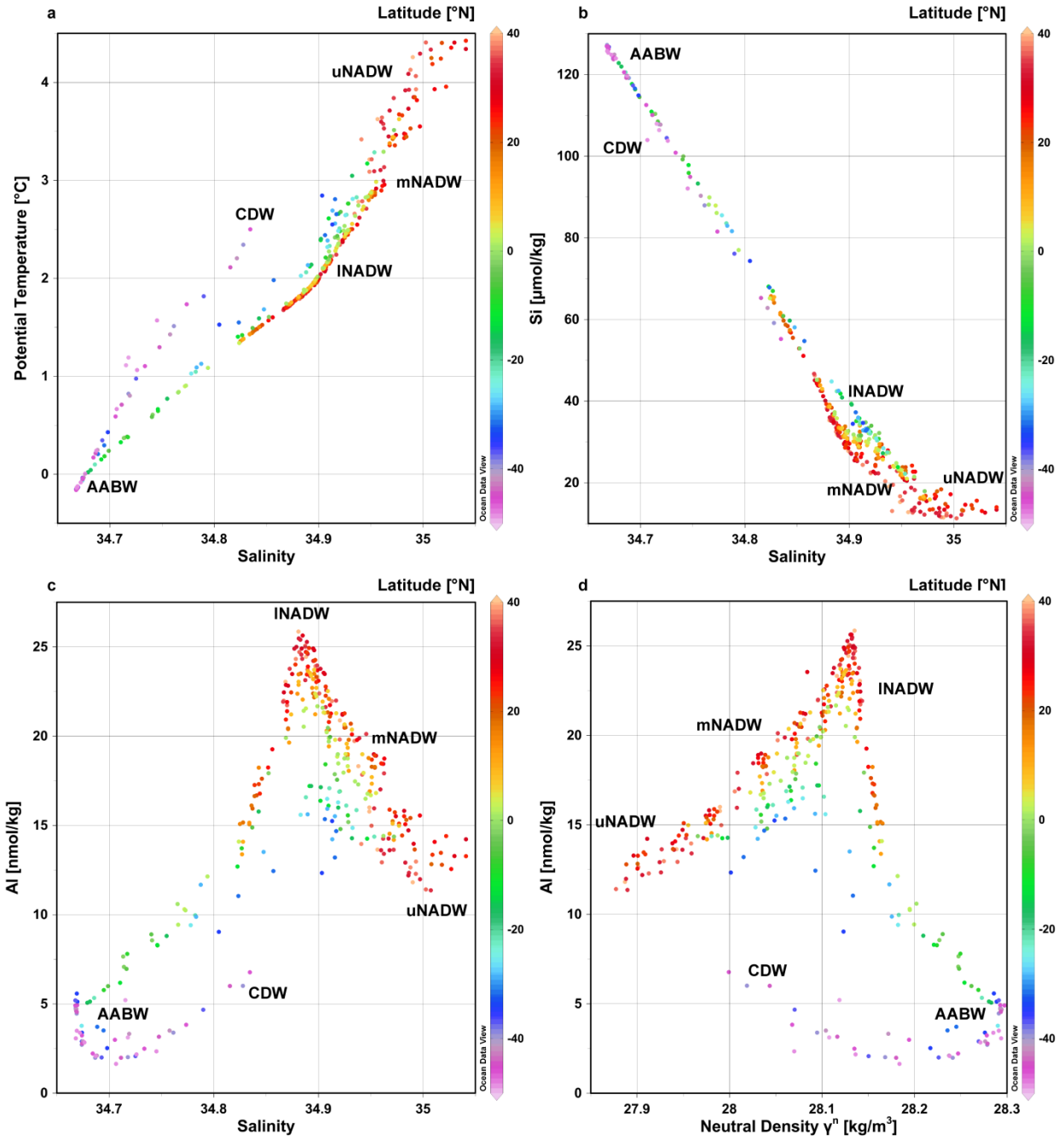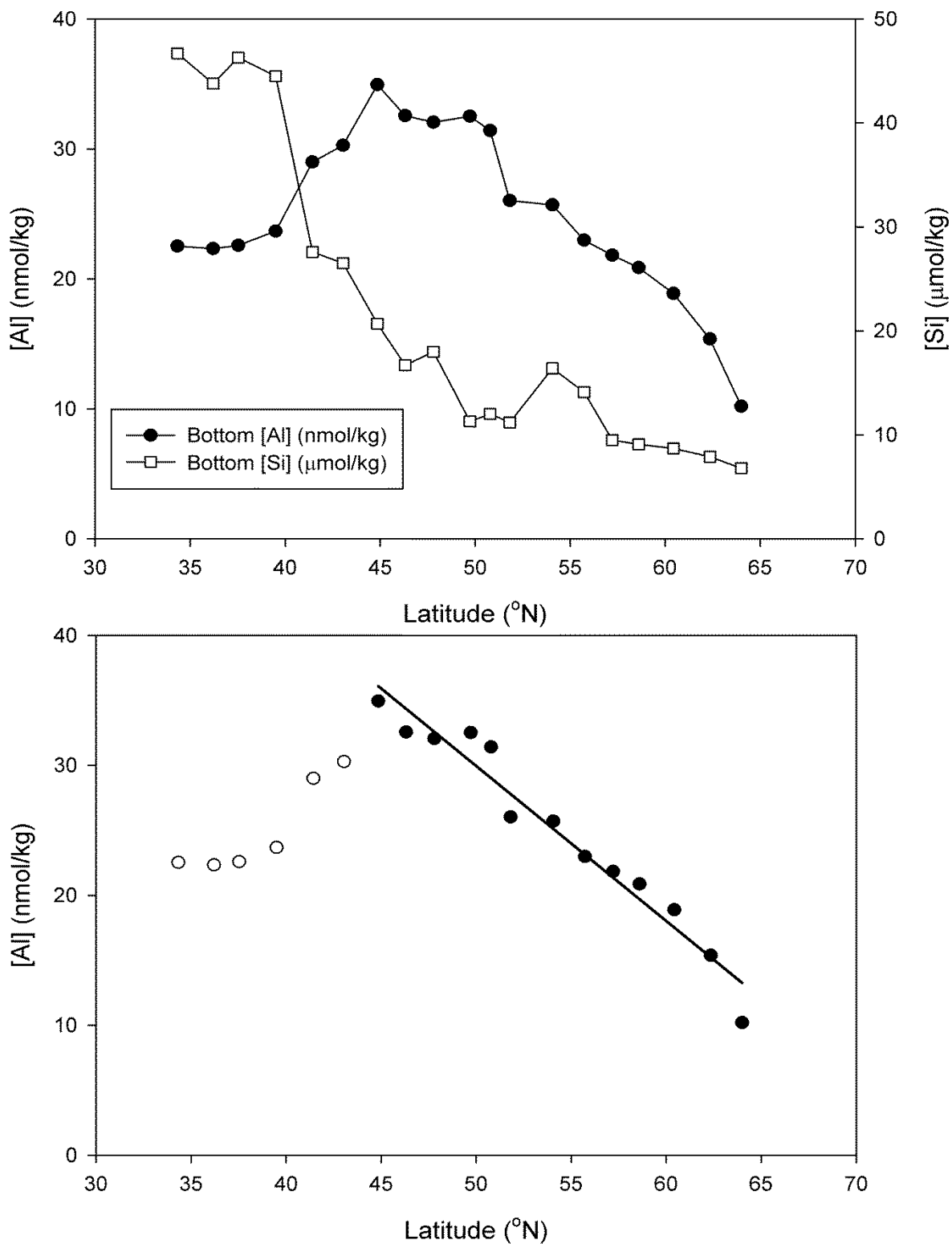Axis labels: [Al] (nmol/kg) (vertical), [Si] (μmol/kg) (horizontal)
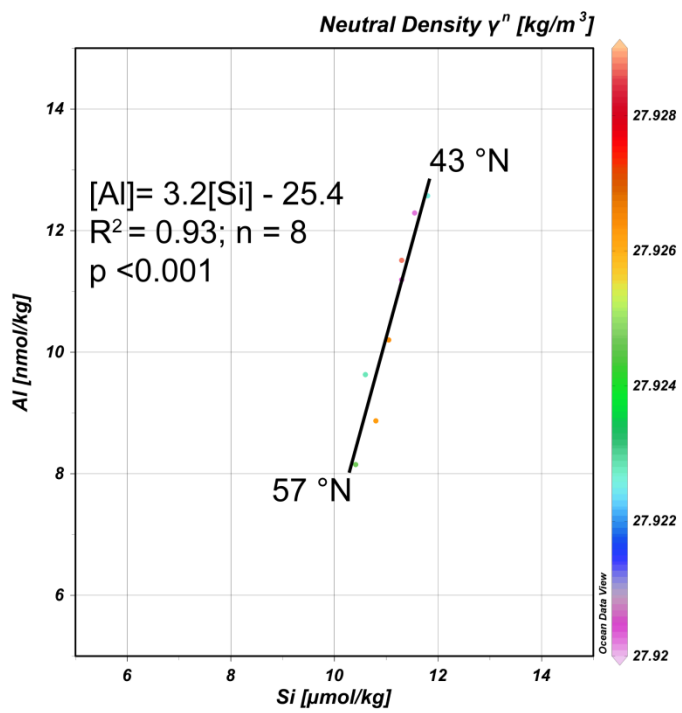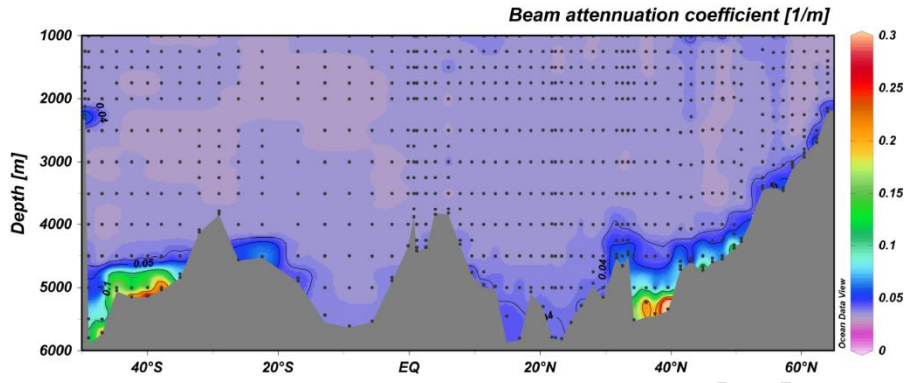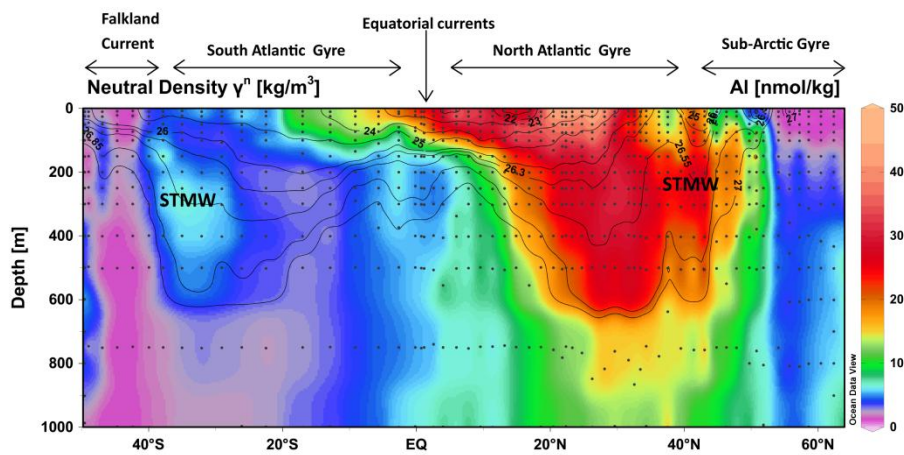
Fig. 7a
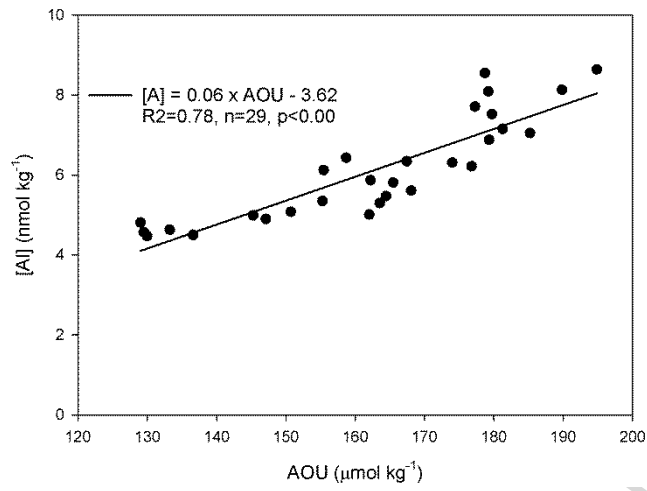
Fig. 7b

Fig. 8

Fig. 9

Fig. 10

Fig. 11

Highlights

- We analysed 1439 samples for dissolved Al along GEOTRACES section GA02
- High Al concentrations where observed in NADW due to sediment resuspension
- Antarctic origin waters are depleted in Al
- High surface Al concentrations have little influence on the deep water distribution
- The distribution of Al can be explained by the combination of its input sources and interaction with biogenic particles